Available online at www.sciencedirect.com
SCIENCE DIRECT
Coordination Chemistry Reviews 250 (2006) 1451–1470
COORDINATION CHEMISTRY REVIEWS
www.elsevier.com/locate/ccr

Review

Some guidelines for the design of anion receptors

Valeria Amendola, Marco Bonizzoni, David Esteban-Gómez [1], Luigi Fabbrizzi *, Maurizio Licchelli, Felix Sancenón [2], Angelo Taglietti

Dipartimento di Chimica Generale, Università di Pavia, via Taramelli 12, I-27100 Pavia, Italy

Received 24 October 2005; accepted 10 January 2006
Available online 10 March 2006

Contents

Abstract

Anions can be recognized by either positively charged or neutral artificial receptors. Positive charges within receptor's cavity can be provided by transition metal ions (e.g. Cu^{II}), which offer a binding site to one donor atom of the envisaged anion. Dicopper(II) bistren cryptates are ideal receptors for ambidentate anions, capable to bridge the two Cu^{II} centres: the size of the ellipsoidal cavity and consequent inclusion selectivity can be modulated by varying the length of the spacers linking the two tren subunits. Examples are discussed of the selective recognition of halides, polyatomic anions, aromatic and aliphatic dicarboxylates. Among neutral receptors, attention is centred to systems containing the urea subunit. Urea behaves as a bifurcate H-bond donor towards oxoanions. On the basis of equilibrium studies in aprotic solvents (mainly MeCN and DMSO), it is shown that the energy of the hydrogen bonding interaction and selectivity are solely related to the acidic tendencies of the receptor and to the basic properties of the anion. In particular, the H-bond interaction can be conveniently viewed as a more or less advanced (and 'frozen') proton transfer from the ─N─H fragment of urea and the oxygen atom of the anion. Addition of excess fluoride may induce deprotonation of the ─NH fragment, essentially due to the unique stability of the $[HF_2]^-$ self-complex which forms.

Keywords: Anion receptors; Oxoanions; H-bond

1. Introduction

There exists a general interest in the design of molecular systems (receptors) capable to selectively interact with anions and possibly to signal to the operator the occurrence of the recognition process (sensors). Lehn and co-workers [1] and Schmidtchen [2] pioneered the field, developing sophisticated

* Corresponding author. Tel.: +39 0382 987328; fax: +39 0382 528544.
E-mail address: luigi.fabbrizzi@unipv.it (L. Fabbrizzi).
[1] Present address: Departamento de Química Fundamental, Universidade da Coruña, A Coruña, Spain.
[2] Present address: Departamento de Química, Universidad Politecnica de Valencia, Valencia, Spain.

0010-8545/$ – see front matter © 2006 Elsevier B.V. All rights reserved.
doi:10.1016/j.ccr.2006.01.006

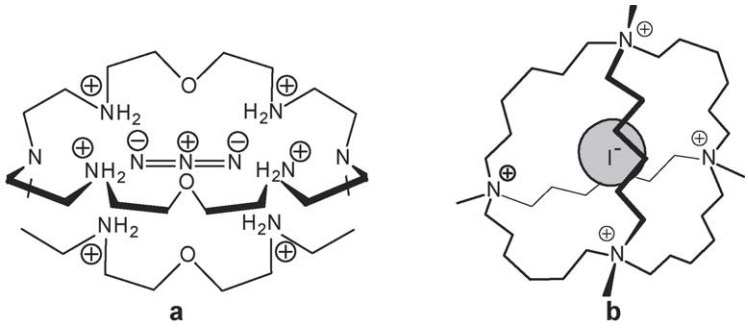

Fig. 1. Prototypes of concave positively charged receptors suitable for anion inclusion. Selectivity is determined by the matching of anion size and cavity dimensions. The receptor–anion interaction is typically electrostatic. Corresponding crystal structures: **a**, ref. [3]; **b**, ref. [4].

positively charged concave receptors, capable of including inorganic anions. Pertinent examples of receptor–anion complexes are shown in Fig. 1. In both cases, the receptor contains positively charged groups (**a**: six ammonium groups, the rod-like azide anion is included in the ellipsoidal cavity [3]; **b**: four tetraalkylammonium groups, the spherical iodide anion is included within the spherical cavity [4]), strategically positioned within the internal framework. Selectivity derives from the matching of the geometrical features (shape, size) of receptor's cavity and of the anion.

Since then, a new branch of chemistry developed, which has been defined *anion coordination chemistry* [5]. In fact, it is formally similar to the classical coordination chemistry of metals, in the sense that it is based on non-covalent interactions and that the object to be coordinated (anion, metal ion) establishes multi-point interactions with the ligating system (receptor, ligand). Very interestingly, some concepts and paradigms of metal coordination chemistry (e.g. the chelate effect, the macrocyclic effect) apply well to anion coordination chemistry. Receptors can be positively charged, not only for the presence of ammonium/tetraalkylammonium fragments, but also due to incorporated metal ions. Receptors can be neutral, too: in that case, they should interact with the anion through hydrogen bonding and should contain H-bond donor groups, essentially N–H fragments from amides and ureas. The classification of anion receptors on the basis of the nature of the interaction is summarized in Scheme 1.

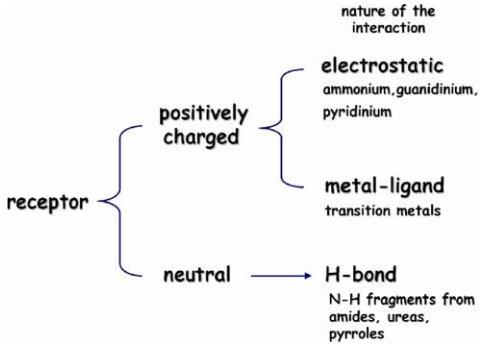

Scheme 1. Electrical state of anion receptors and nature of the receptor–anion interaction.

In the past decade, we have considered the design of a variety of receptors for anions, both inorganic and organic, and for some ionizable analytes, in particular amino acids, by taking profit from the varying types of interaction illustrated in Scheme 1. The development of this chapter follows the temporal progress of our research efforts, from receptors operating through metal–ligand interactions (an approach reflecting our cultural background in transition metal coordination chemistry), to neutral, purely organic receptors, in particular: ureas.

Excellent reviews have been published during the last years which have clearly outlined the principles of anion recognition [6–16], and new observations on the same topic are being currently reported by numerous Laboratories. The present article is not aimed to update and comment specific literature, but to provide an account of our own work in the field and to express some general considerations which originated from it and which we would like to share with the wider community of people interested on anion chemistry.

2. Anion recognition based on the metal–ligand interaction

2.1. Bistren cryptates: halide recognition

Anions typically form complexes with metal ions, whose stability may vary depending upon the electronic features of the ligand and of the metal centre and can be interpreted on the basis of traditional classifications (e.g. hard and soft theory). However, selectivity cannot be merely founded on metal–ligand affinity. Rather, the metal should simply provide a single binding site, whereas selectivity could be associated to the geometrical and steric characteristics of the receptor (ligand), in which the metal is incorporated. The tetraamine tren provides a suitable coordinative environment: it imposes a trigonal bipyramidal geometry to most metal ions, leaving an axial site available for anion (or solvent) binding. In order to increase steric constraints and enhance selectivity, two tren subunits can be linked together through three spacers [17], to give a cage (**3**). The bistren cage **3** can incorporate two metal ions (e.g. Cu^{II}), to give the homodimetallic complex **4**. Then, an ambidentate anion X^- can bridge the two metal centres, thus forming the ternary inclusion complex **5**. The so-called *cascade* process is illustrated in Fig. 2.

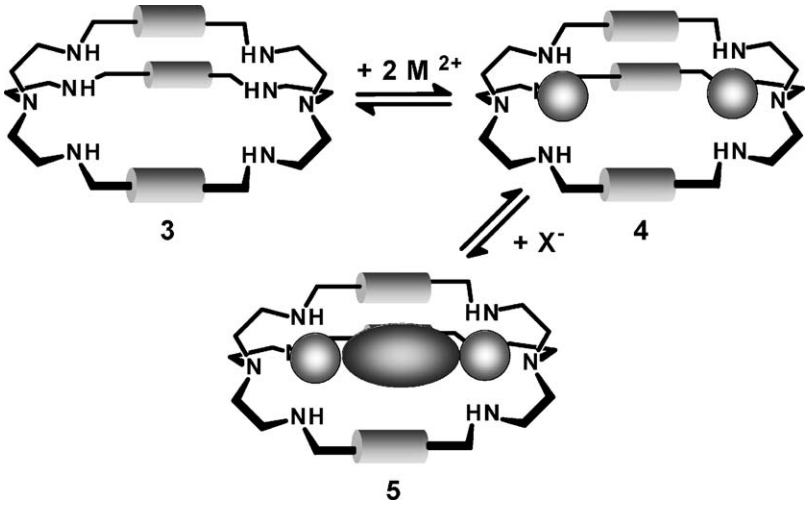

Fig. 2. A cascade process for the inclusion of an anion X^- into a bistren homodimetallic cage. The anion must be ambidentate, e.g. Cl^-, NCO^-, $^-OOC{-}R{-}COO^-$, and should bridge the two metal centres. The inclusion selectivity derives from the matching of the anion dimensions and the size of bistren cavity, which is ultimately related to the length of the spacers.

Following the nomenclature introduced by Lehn [18], the bistren cage **3** can be defined as a *cryptand*, and complex **4** a *cryptate*. Thus, the supramolecular complex **5** should be classified as a *supercryptate*. We have considered a variety of cryptands, differing in the nature of the spacers and suitable for the inclusion of ambidentate anions of varying type and length. In most cases, anion inclusion has been definitively demonstrated by X-ray structures on isolated supercryptates [19]. Most interestingly, selective affinity towards anions has been assessed in aqueous solution, by titrating a solution of the cryptate with a standard solution of the envisaged anion [20].

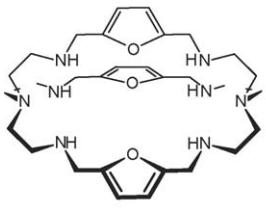
6

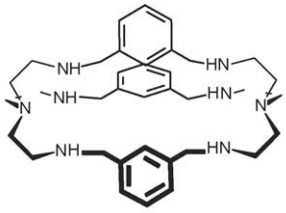
7

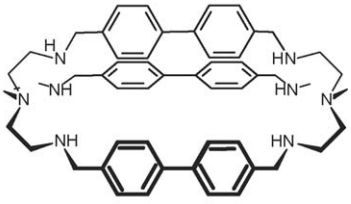
8

The dicopper(II) cryptate **6** forms stable inclusion complexes with halides. Fig. 3 shows the structure of the bromide complex: $[Cu_2^{II}(\mathbf{6})(Br)]^{3+}$ [21]. The halide anion is encapsulated within the cage and bridges the two metal centres. Both metal ions exhibit a compressed trigonal bipyramidal stereochemistry and are slightly displaced from the equatorial plane of the three secondary amine nitrogen atoms of each tren subunit, towards the halide ion. The Cu–Cu distance is 4.86 Å and the Cu–Br–Cu angle is 179.4°.

Before assessing selective affinities toward anions, one must first define the state of the receptor in the chosen medium. In this sense, the formation of the cryptate complex in aqueous solution was investigated through potentiometric titration [21]. In a typical experiment, a solution containing **6**, 2 equiv. of $Cu^{II}(CF_3SO_3)_2$ plus excess acid was titrated with standard base. On non-linear least-squares treatment of titration data, the equilibrium constants pertinent to the species present at the equilibrium were evaluated and their distribution diagram, over the investigated range of pH, was drawn (see Fig. 4).

Two major metal complex species are present, along the investigated range of pH: $[Cu_2L]^{4+}$, which reaches its maximum concentration (90%) at pH 5, and $[Cu_2L(OH)]^{3+}$, almost 100%, at pH 8–9. It is suggested that in the $[Cu_2L]^{4+}$ cryptate a water molecule is axially coordinated to each Cu^{II} centre, completing the trigonal bipyramidal polyhedron. On the other hand, the $[Cu_2L(OH)]^{3+}$ complex has been characterized in its crystalline form: the oxygen atom of the hydroxide ion bridges the two Cu^{II} centres [22].

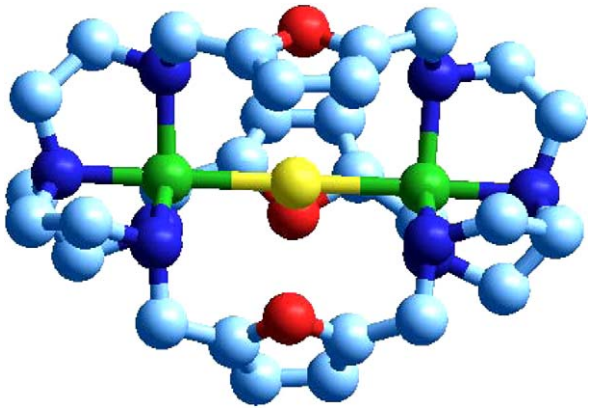

Fig. 3. The structure of the $[Cu_2^{II}(\mathbf{6})(Br)]^{3+}$ supercryptate. The bromide ion bridges the two Cu^{II} centres. Each Cu^{II} ion experiences an axially compressed trigonal bipyramidal geometry, typically observed in tren and bistren complexes.

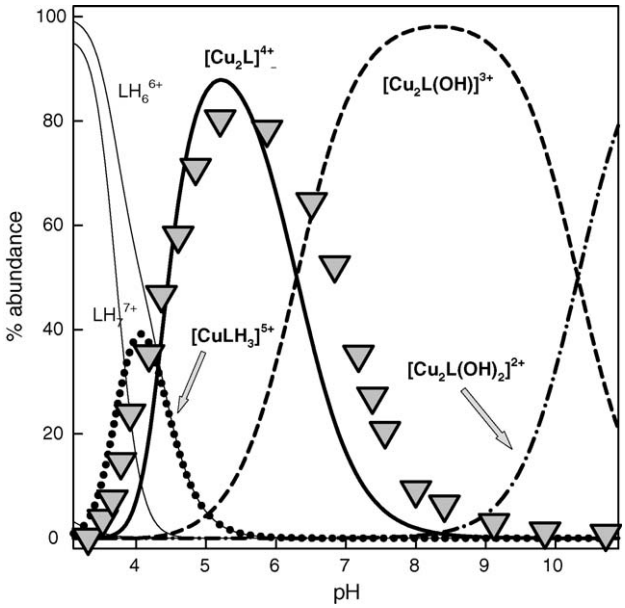

Fig. 4. %Concentration of the species present at the equilibrium for the system **6**/Cu^{II} (ligand-to-metal ratio 1:2), in an aqueous solution 0.1 M in $NaClO_4$, at 25 °C. Triangles indicate the absorbance of the band centred at 410 nm, measured in presence of a 10-fold excess of Cl^- (pertinent to the yellow $[Cu_2^{II}(\mathbf{6})(Cl)]^{3+}$ supercryptate; arbitrary values; limiting value of molar absorbance is 12,600 M^{-1} cm^{-1}).

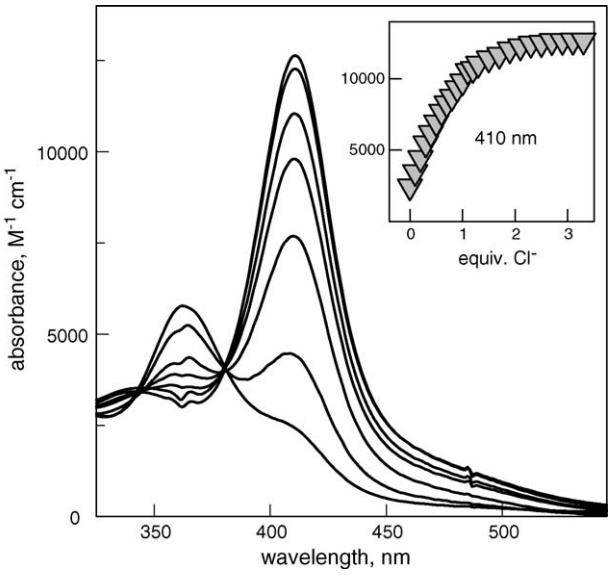

Fig. 5. Titration with Cl^- of a solution containing the $[Cu_2^{II}(\mathbf{4})]^{4+}$ cryptate complex, adjusted to pH 5.25 (0.05 MES buffer). The increasing band centred at 410 nm corresponds to the formation of the $[Cu_2^{II}(\mathbf{6})(Cl)]^{3+}$ inclusion complex. Non-linear least-squares treatment of the titration profile in inset gave a log K value of 3.98 ± 0.02 for the equilibrium: $[Cu_2^{II}(\mathbf{6})]^{4+} + Cl^- \leftrightarrows [Cu_2^{II}(\mathbf{6})(Cl)]^{3+}$.

We considered that the $[Cu_2^{II}L]^{4+}$ complex, with its 'empty' cavity, could represent the ideal receptor to evaluate binding tendencies of halide ions in water. Thus, a solution was buffered to pH 5.2, the pH at which the $[Cu_2^{II}L]^{4+}$ cryptate was present at the highest concentration, and was titrated with sodium halides. For instance, on addition of chloride, the pale blue solution of the $[Cu_2^{II}L]^{4+}$ complex became bright yellow, while a very intense band developed at 410 nm. The family of spectra that developed over the course of the titration is shown in Fig. 5. The titration profile shown in the inset (absorbance at 410 nm versus equiv. of Cl^-) indicated the formation of a 1:1 cryptate/chloride supercomplex. Non-linear least-squares treatment of the data of the spectrophotometric titration experiment gave a log K value of 3.98 ± 0.02. Similar behaviour was observed when the pale blue solution of the 'empty cavity' complex, $[Cu_2^{II}L]^{4+}$, was titrated with standard bromide and iodide solutions: a bright yellow colour formed and an intense band developed above 400 nm (Br^-: λ_{max} = 430 nm, ε = 10,800 M^{-1} cm^{-1}; I^-: λ_{max} = 440 nm, ε = 950 M^{-1} cm^{-1}). log K values for the 1:1 cryptate/halide supercomplex were 3.01 ± 0.01 for bromide and 2.39 ± 0.02 for iodide. Titration with NaF did not cause any development of the yellow colour. However, this did not exclude the formation of the inclusion complex of fluoride. In fact, the rather strong absorption band observed for Cl^-, Br^- and I^- has a halide-to-metal charge transfer (CT) character, and its energy must increase with the increasing electronegativity of the halogen atom. Thus, the CT transition for the $[Cu_2^{II}(\mathbf{6})(F)]^{3+}$ complex, due to the high electronegativity of fluorine, should be shifted to the UV portion of the spectrum, where it may be obscured by the strong amine-to-metal CT transitions. However, significant spectroscopic modifications in the UV region were observed when titrating with NaF the cryptate solution buffered at pH 5.2; in particular, a saturation 1:1 profile was obtained and the value of log K could be determined: 3.20 ± 0.02.

If log K values are plotted versus halide ion radius, a defined selectivity pattern in favour of chloride is observed (see Fig. 6). Notice that the anion size effect is rather moderate, ranging within an interval of 1.2 log units. It is possible that it is not determined by steric factors, but simply reflects the coordinating tendencies of halide ions towards transition metals (i.e. their position in the spectrochemical series: $Cl^- > F^- > Br^- > I^-$).

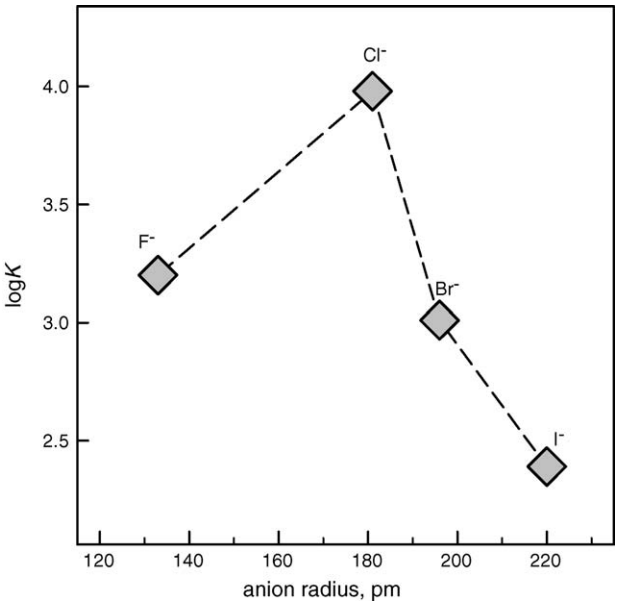

Fig. 6. Selectivity pattern for the inclusion equilibrium: $[Cu_2^{II}(\mathbf{6})]^{4+} + X^- = [Cu_2^{II}(\mathbf{6})(X)]^{3+}$ equilibrium (X^- = halide anion, aqueous solution, buffered at pH 5.2).

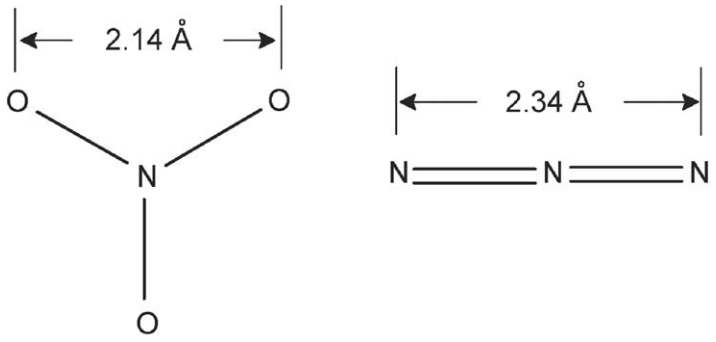

Fig. 7. The 'bite length' of ambidentate anions (i.e. the distance between two consecutive donor atoms). In rod-like anions like N_3^- the bite coincides with the length of the anion.

Notably, the cryptate $[Cu_2^{II}(\mathbf{6})]^{4+}$ is able to include also non-spherical anions, like the rod-like triatomic anions N_3^- ($\log K = 4.70 \pm 0.06$) and NCS^- ($\log K = 4.28 \pm 0.03$), which require an ellipsoidal cavity. Notice that on addition of OH^- to $[Cu_2^{II}(\mathbf{6})]^{4+}$, i.e. simply moving from pH 5.2 to pH 8, the emerald green complex $[Cu_2^{II}(\mathbf{6})(OH)]^{3+}$ forms, in which the oxygen atom of the hydroxide ion bridges the two Cu^{II} centres. The Cu–Cu distance in the hydroxide complex, evaluated from the crystal structure [22], is 3.90 Å, to be compared with the distance observed in the $[Cu_2^{II}(\mathbf{6})(Br)]^{3+}$ supercryptate (4.86 Å). The intermetallic distance must be remarkably larger in the corresponding azide and thiocyanate inclusion complexes (but no X-ray structures are available). Thus, it appears that the $[Cu_2^{II}(\mathbf{6})]^{4+}$ complex displays an extreme versatility, being capable of reducing and expanding its cavity in order to include anions of variable size and shape, from the small hydroxide to the large thiocyanate. However, flexibility and versatility may enrich anion coordination chemistry, but surely contrast selectivity in anion recognition.

2.2. Bistren cryptates: recognition of polyatomic anions

Well-defined steric effects are observed in the case of the dicopper(II) complex of cryptand **7**, in which the two tren subunits are linked by 1,3-xylyl spacers [23]. Anion inclusion studies were carried out in an aqueous solution buffered at pH 7, where the cryptate exists mainly as $[Cu_2^{II}(\mathbf{7})OH]^{3+}$, as found from pH titration experiments. In the pale blue complex, the two available axial positions are occupied by an hydroxide ion on one metal centre and by a water molecule on the other. The rigidity of the cryptand framework, imparted by the 1,3-xylyl spacers, prevents the shrinking of the cavity and the bridging of the two Cu^{II} ions by the hydroxide ion, as observed in the $[Cu_2^{II}(\mathbf{6})OH]^{3+}$ cryptate. In any case, both OH^- and H_2O are not firmly bound to the Cu^{II} centres and can be easily replaced by an ambidentate anion. In fact, inclusion is observed with a variety of polyatomic anions of varying geometry: linear (N_3^-, NCO^-, NCS^-), triangular (NO_3^-), Y-shaped (HCO_3^-, CH_3COO^-) and tetrahedral (SO_4^{2-}). Apparent constants of the inclusion equilibrium (at pH 7.0) span two orders of magnitude, from N_3^- (highest affinity) to NCS^- (lowest affinity). Neither shape nor size of the anion determines inclusion selectivity. The key geometrical parameter is the *bite length*, i.e. the distance between two consecutive donor atoms of the anion. Bite length is visually defined in Fig. 7.

In particular, if $\log K$ values are plotted versus bite length (see Fig. 8), a sharp *peak selectivity* pattern is observed: the linear N_3^- and NCO^- ions and the Y-shaped HCO_3^- anion show the highest affinity because their bite fits well the distance between the available axial sites of the two Cu^{II} centres, within the cryptate relaxed to its more stable conformational arrangement. Inclusion of anions of larger or smaller bite length induces an endoergonic rearrangement of the cryptand's framework, which is reflected in a decrease of the binding constant. Geometrical effects overcome factors related to anion coordinative tendencies. Just to make an example, in the absence of steric constraints, NCS^- typically shows higher binding tendencies towards copper(II) tetraamine complexes than N_3^-.

Anion recognition by the dimetallic cryptate at pH 7 is signalled by a colour change, from the pale blue $[Cu_2^{II}(\mathbf{7})OH]^{3+}$ species to the blue-green inclusion complex $[Cu_2^{II}(\mathbf{7})X]^{3+}$: colour results from a rather intense LMCT band at ca. 400 nm. However, anion recognition can be more sensitively signalled by a change of the fluorescent emission, by taking profit of

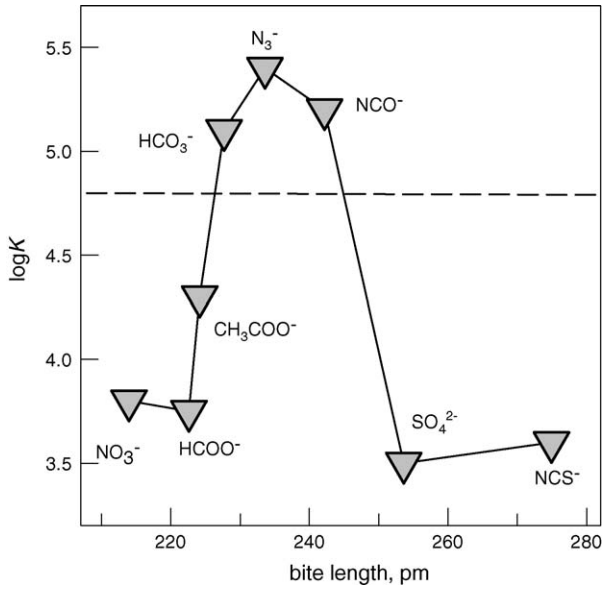

Fig. 8. Peak selectivity in the inclusion of polyatomic anions by the $[Cu_2^{II}(\mathbf{7})]^{4+}$ cryptate. The dimetallic receptor does not recognise the shape of the anion, but its *bite*, i.e. the distance between two consecutive donor atoms.

the *indicator displacement paradigm* [24–27] According to this approach, a receptor R interacts with a fluorescent indicator I, to give a fairly stable adduct [R·I], in which the emission of I is quenched through an intra-complex process (of either electron transfer, eT, or energy transfer, ET, nature). Then, the envisaged analyte X is added, and this displaces I and forms a more stable complex with R: when released to the solution, I can display its fluorescent emission, thus signalling the recognition of X by R. The overall process is described by the following equilibria (superscript (⋆) indicates fluorescence):

$$R + I^{\star} \leftrightarrows [R{\cdot}I] \qquad K_I \qquad (1)$$

$$[R{\cdot}I] + X \leftrightarrows [R{\cdot}X] + I^{\star} \qquad K_d \qquad (2)$$

$$R + X \leftrightarrows [R{\cdot}X] \qquad K_X = K_d \times K_I \qquad (3)$$

In a preliminary experiment, $I^{\star}$ is titrated with R and, from the titration profile (quenching of fluorescence), K_I is calculated. Then a solution containing R and I (which is present at a much lower concentration, just as an indicator) is titrated with X and, from the titration profile (revival of fluorescence), K_d is determined. Then, K_X can be calculated: $K_X = K_d \times K_I$.

The paradigm described above has been successfully used for the fluorimetric detection of carbonate in mineral waters, using $[Cu_2^{II}(\mathbf{7})OH]^{3+}$ as a receptor R [16].

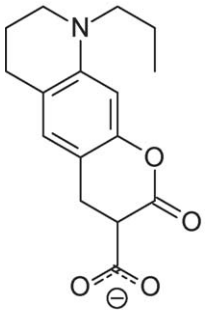

9

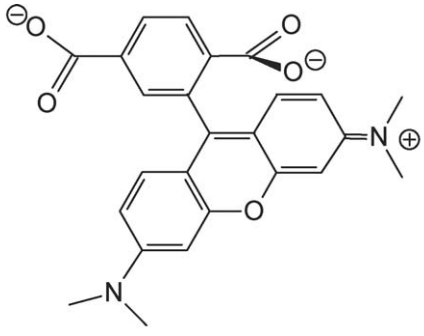

10

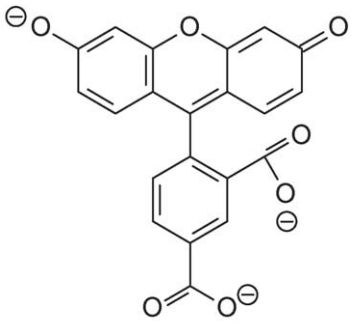

11

As a fluorescent indicator we chose coumarine 343 (**9**, C^-), which possesses a carboxylate function capable of bridging the two Cu^{II} centres of receptor $[Cu_2^{II}(\mathbf{7})]^{4+}$. Coumarine 343 is strongly fluorescent also in its anionic form, which is the dominating species in an aqueous solution adjusted to pH 7. Complete quenching of the coumarine emission was observed ($\lambda_{exc} = 424$ nm, $\lambda_{em} = 487$ nm), on titrating a degassed solution of **9** (10^{-7} M), buffered to pH 7, with a standard solution of the receptor: a value of $\log K_I = 4.8 \pm 0.1$ was calculated from the spectrofluorimetric titration profile. Such a value is indicated as a horizontal dashed line in Fig. 8. Quenching has to be ascribed to the occurrence of an eT or ET process between the copper(II) centre(s) and the excited fluorophore. Thus, in a titration experiment in which the anion X^- is added to a solution containing $[Cu_2^{II}(\mathbf{7})]^{4+}$ and the indicator C^-, only anions whose $\log K$ is above the dashed line (NCO^-, N_3^-, HCO_3^-) will be able to displace the indicator from receptor's cavity, an event which is signalled by the revival of coumarine emission. Anions whose $\log K$ lies below the dashed line will be discriminated. Fig. 9 shows how, following this protocol, HCO_3^- can be discriminated from other common anions.

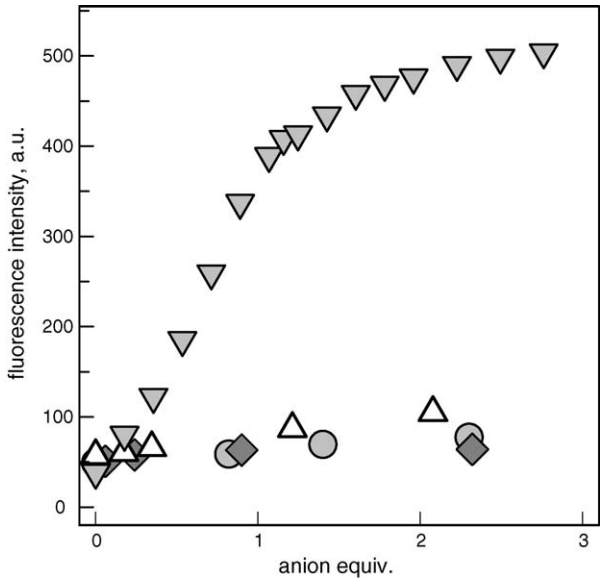

Fig. 9. Titration of an aqueous solution containing $[Cu_2^{II}(\mathbf{7})]^{4+}$, 2×10^{-4} M, and coumarine 343, **9**, 10^{-7} M, buffered to pH 7, with standard solutions of selected anions. Only HCO_3^- (triangles down) is able to displace the indicator from the cryptate receptor, making coumarine fluorescence revive. Other anions, e.g. phosphate (triangles up), acetate (circles) and sulphate (diamonds) do not compete successfully and induce only a slight fluorescence enhancement.

Moreover, on the basis of a calibration curve, a substantial range of carbonate concentrations could be explored, covering all the commercially available mineral waters [23]. Such a methodology is easier and more selective than that currently used, which is based on the volumetric titration of the alkalinity with standard hydrochloric or sulphuric acid; in particular, the latter procedure cannot distinguish HCO_3^- ions from other basic solutes present in solution.

2.3. Bistren cryptates with long spacers: recognition of dicarboxylates, including glutamate

Bistren cryptand **8**, containing ditolyl spacers, offers a much longer ellipsoidal cavity and is suitable for the inclusion of anions whose negatively charged groups are distinctly sepa-

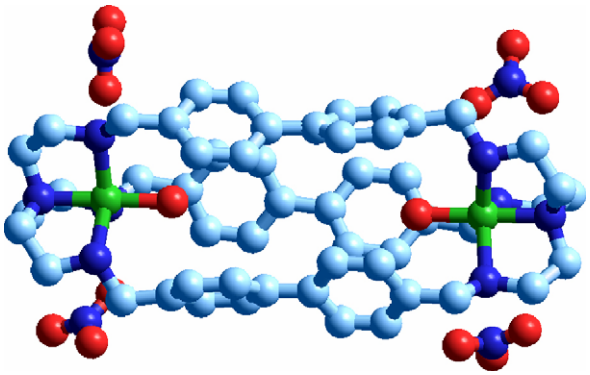

Fig. 10. The crystal structure of the $[Cu_2^{II}(\mathbf{8})(H_2O)_2](NO_3)_4$ cryptate salt. No nitrate ion is included within the cryptate cavity, which contains two water molecules coordinated to the Cu^{II} centres.

rated (e.g. dicarboxylates). The dicopper(II) cryptate of **8** was isolated as a tetranitrate salt and crystallographically characterized [28]: quite interestingly, the cavity does not contain any nitrate ion, but two water molecules, each one coordinated to a Cu^{II} centre, to complete five-coordination (according to a compressed trigonal bipyramidal geometry, see the structure in Fig. 10).

We investigated cryptate $[Cu_2^{II}(\mathbf{8})(H_2O)_2]^{4+}$ as a receptor for a variety of dicarboxylates, both aromatic and aliphatic. It is assumed that the structure of the $[Cu_2^{II}(\mathbf{8})(H_2O)_2]^{4+}$ complex reflects the most relaxed and minimum energy conformation of the cryptate. Thus, in the ideal dicarboxylate for inclusion, two oxygen atoms of the two carboxylate groups should exhibit the same distance as that between the oxygen atoms of the two water molecules in the $[Cu_2^{II}(\mathbf{8})(H_2O)_2]^{4+}$ cryptate: 7.36 Å. This condition would allow anion inclusion without any endoergonic rearrangement of the cryptate backbone.

The interaction of $[Cu_2^{II}(\mathbf{8})(H_2O)_2]^{4+}$ with dicarboxylates was investigated in water, at pH 7, using the fluorescent indicator displacement paradigm. Such an approach was adopted in view of the rather low solubility of the cryptate complex ($\leq 10^{-5}$ M): in particular, the use of a powerful fluorescent probe would allow monitoring of anion inclusion even at rather low concentration levels. As a fluorescent indicator, we chose a rhodamine based indicator (**10**), which contains a 1,4-benzene-dicarboxylate moiety, suitable for bridging the two Cu^{II} centres within receptor's cavity. Rhodamine, when excited at 496 nm (isosbestic point), emits at 571 nm (orange fluorescence). On titrating an aqueous solution 2.5×10^{-7} M in **10** and buffered to pH 7 with HEPES with a standard solution of the cryptate complex, a progressive decrease of the fluorescence intensity I_F of **10** was observed, until complete quenching (see Fig. 11). From non-linear fitting of the titration profile (shown in Fig. 11, inset), an inclusion constant log K of 7.0 ± 0.2 was calculated. The rather high value of the constant suggests that the two $-COO^-$ groups of the indicator coordinate the two Cu^{II} centres, which quench the proximate fluorophore through either an eT or an ET process.

Then, a solution containing the cryptate complex $[Cu_2^{II}(\mathbf{8})]^{4+}$ (2.5×10^{-6} M) and the indicator **10** (2.5×10^{-7} M) was titrated with a selection of dicarboxylates.

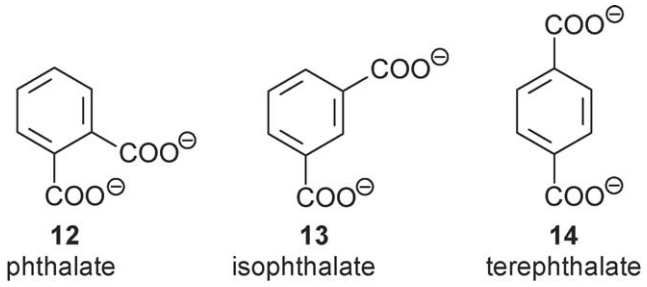

First, it is interesting to consider the behaviour of the positional isomers of phthalate (1,2: phthalate, **12**; 1,3: isophthalate, **13**; 1,4: terephthalate, **14**). Corresponding titration profiles are shown in Fig. 12.

Only the 1,4-derivative (terephthalate) is capable of displacing the rhodamine indicator from the cavity of the cryptate, whereas the other two isomers do not compete successfully. Such a discriminating behaviour can be fully explained on the basis of geometrical and structural reasons. In fact, the distance between two opposite oxygen atoms in the terephthalate ion, as observed in the X-ray determined structure of an ammonium salt, is 7.39 Å, which fits quite well the distance between water oxygen atoms in the cryptate complex (7.36 Å). Thus, it appears that the terephthalate ion has an almost ideal O···O bite to bridge the two Cu^{II} centres without inducing any endoergonic rearrangement of the cage framework. In contrast, serious rearrangement must occur with the inclusion of isophthalate and phthalate ions, whose O···O distances, as observed in the X-ray determined structures of the ammonium salts, are distinctly smaller (4.98 and 3.16 Å, respectively). Notice that rhodamine itself possesses the benzene-1,4-dicarboxylate fragment, which ensures the most favourable fit. However, its inclusion constant is one order of magnitude lower than that for terephthalate, probably due to repulsive effects exerted by the bulky fluorogenic fragment (of steric nature) and by the positive charge

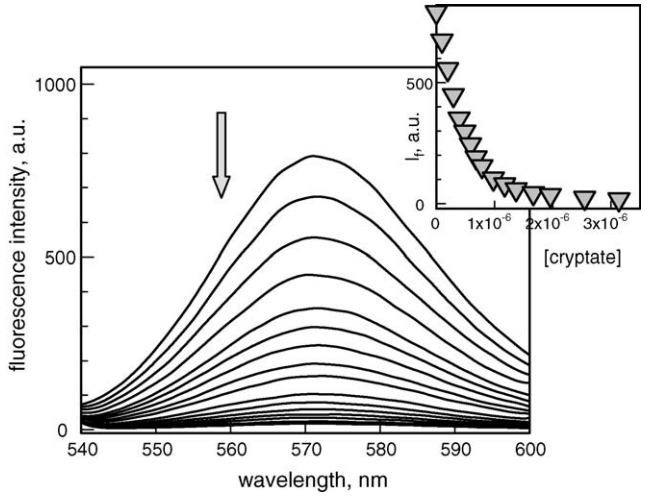

Fig. 11. Titration of an aqueous solution of rhodamine, **10**, 2.5×10^{-7} M, buffered to pH 7, with a standard solution of $[Cu_2^{II}(\mathbf{8})]^{4+}$. The dicopper(II) cryptate includes the dicarboxylate moiety of the indicator and quenches the fluorophore. From the titration profile in the inset, an inclusion constant log $K = 7.0 \pm 0.2$ was calculated.

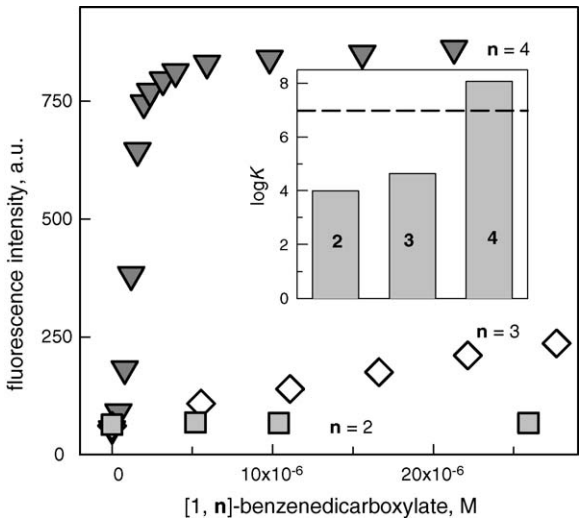

Fig. 12. Titration of a solution 2.5×10^{-6} M in $[Cu_2^{II}(\mathbf{8})]^{4+}$ and 2.5×10^{-7} M in **10** with 1,*n*-benzene-dicarboxylates in an aqueous solution buffered at pH 7. Triangles: $n = 4$; diamonds: $n = 3$; squares: $n = 2$. In the bar diagram in the inset, the inclusion constants for the three dicarboxylates are reported. The dashed line corresponds to the log *K* value for the inclusion into the cryptate of the rhodamine indicator **10**, and defines recognition selectivity.

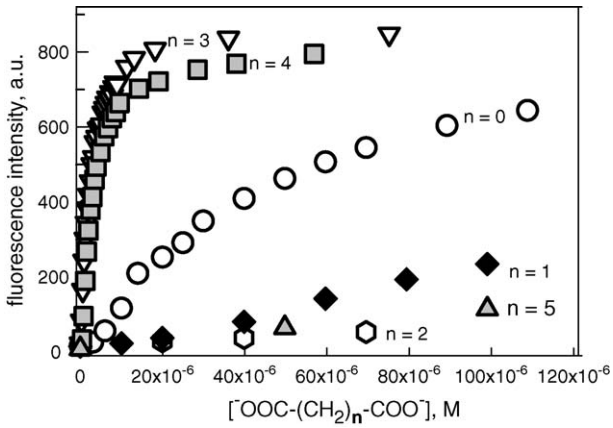

Fig. 13. Titration of a solution 2.5×10^{-6} M in $[Cu_2^{II}(\mathbf{8})]^{4+}$ and 2.5×10^{-7} M in **10** with aliphatic dicarboxylates of formula $^{-}OOC(CH_2)_nCOO^{-}$ ($n = 0$–5), in an aqueous solution buffered at pH 7.

on the fluorophore (electrostatic). The corresponding inclusion constants were calculated through non-linear least-squares analysis of titration experiments and their values are reported as a bar diagram in the inset of Fig. 12. The diagram illustrates well the efficiency of the indicator displacement paradigm: the log *K* of the indicator is lower than that of the analyte of interest (terephthalate), but distinctly higher than those of the interferents (isophthalate and phthalate).

hand, dicarboxylates with a shorter (succinate, $n = 2$) or longer (pimelate, $n = 5$) carbon chain are not capable of displacing the indicator from the dicopper(II) cryptate, so that the fluorescence of the solution is kept almost quenched.

The inclusion constants for all the dicarboxylates were calculated through non-linear fitting of titration profiles shown in Fig. 13. First, we note that the smaller dicarboxylates oxalate and malonate undergo double stepwise inclusion (oxalate: $\log K_1 = 6.1 \pm 0.3$, $\log K_2 = 3.2 \pm 0.3$; malonate: $\log K_1 = 4.8 \pm 0.3$, $\log K_2 = 3.2 \pm 0.3$). This behaviour is ascribed to the relatively small size of the two anions, which cannot encompass the distance between the two metal

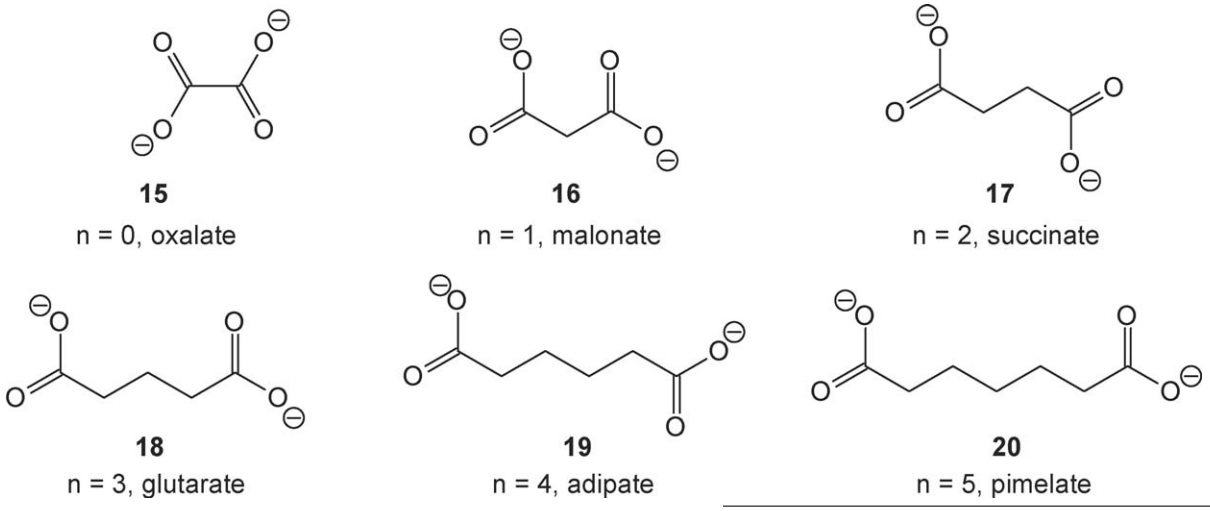

A further class of difunctional anions to be considered was that of aliphatic dicarboxylates, of general formula $^{-}OOC(CH_2)_nCOO^{-}$ ($n = 0$–5). Fig. 13 shows the spectrofluorimetric profiles obtained on titrating a solution 2.5×10^{-6} M in $[Cu_2^{II}(\mathbf{8})]^{4+}$ and 2.5×10^{-7} M in **10**, buffered to pH 7, with standard solutions of aliphatic carboxylates (**15**–**20**).

Sharp selectivity is displayed by glutarate ($n = 3$) and adipate ($n = 4$), which definitively displace the indicator from the receptor, inducing full revival of fluorescence. On the other

centres and prefer individual coordination to each Cu^{II} ion. Inclusion of a single anion is observed with longer dicarboxylates ($n = 2$–5) and corresponding equilibrium constants are reported in Table 1.

Glutarate ($n = 3$) and adipate ($n = 4$) exhibit inclusion constants similar to that of rhodamine: however, they compete successfully for the receptor because they are present in a 10-fold higher concentration than the indicator. Succinate ($n = 2$) and pimelate ($n = 5$) exhibit inclusion constants definitively lower

than that of the indicator and, even if present in 10-fold excess, cannot displace rhodamine from the cryptate. Noticeably, the highest affinity for the receptor is exhibited by glutarate and adipate whose crystallographically determined O···O distances, (d(O···O), see values in Table 1), are the closest to the ideal value of 7.36 Å. Dicarboxylates whose O···O distances deviate remarkably from the ideal value (succinate, $n = 2$; pimelate, $n = 5$) give much less stable inclusion complexes. In particular, the inclusion constants correlate well with Δd(O···O), i.e. the difference between d(O···O) and 7.36 Å.

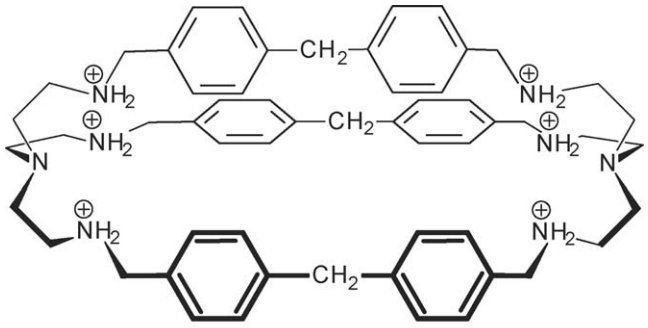

21

Recognition of dicarboxylates by a bistren cage had been previously investigated by Lehn et al., by taking profit from electrostatic interactions [29]. In particular, a solution of the octaamine cryptand **21** in D_2O, adjusted to pH 6, was titrated with standard solutions of aliphatic dicarboxylates of formula $^{-}OOC–(CH_2)_n–COO^{-}$, with $n = 2$–7. At that pH value, the cage is in the form of a hexammonium cation, with the six secondary amine groups protonated. Constants for the inclusion equilibrium ($LH_6^{6+} + A \sim A^{2-} \leftrightarrows [LH_6 \cdot A \sim A]^{4+}$) are plotted versus n, the number of carbon atoms of the aliphatic chain linking the two carboxylate groups in the diagram in Fig. 14.

No pronounced selectively is observed for the inclusion of dicarboxylate whose carbon chain varies to a substantial extent. This behaviour is contrasting with the peak selectivity observed for the cryptate receptor $[Cu_2^{II}(\mathbf{8})]^{4+}$, whose log K value are plotted in the diagram for comparative purposes.

Such a striking difference may be due to: (i) the higher flexibility of the spacers present in cryptand **21** (an sp^3 carbon atom interfaces the two phenyl rings); (ii) the adirectional nature of electrostatic interactions (compared to the strongly directional metal–ligand interactions).

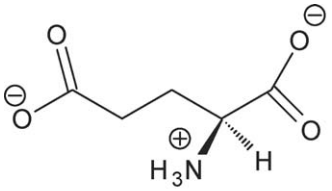

22
L-glutamate

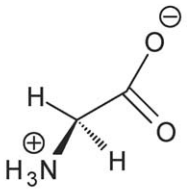

23
glycine

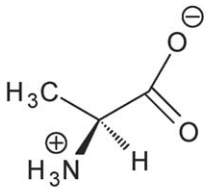

24
L-alanine

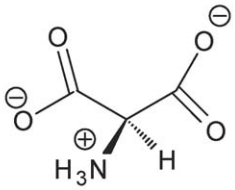

25
L-aspartate

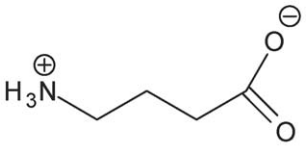

26
γ-aminobutanoate
(GABA)

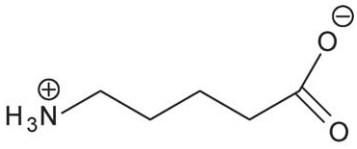

27
δ-aminopentanoate

A biologically relevant dicarboxylate which could be conveniently determined through the spectrofluorimetric procedure described above is L-glutamate (which possesses the same carbon skeleton as glutarate). In fact, L-glutamate is a major excitatory transmitter in the central nervous system and its selective determination in presence of other neurotransmitters is strongly required by neurophysiologists. In particular, they need to determine L-glutamate concentration in real time and real space, using a fluorescence microscope.

The interaction of L-glutamate with $[Cu_2^{II}(\mathbf{8})]^{4+}$ in aqueous solution, at pH 7, was investigated spectrofluorimetrically, using the described procedure [30]: pertinent titration profile is plotted in Fig. 15 and compared with those obtained for other anionic neurotransmitters and related amino acids. L-Glutamate is able to displace the indicator from the cryptate in the same way as glutarate. In particular, its inclusion constant is the same as observed for glutarate (log $K = 6.9 \pm 0.2$). Good discrimina-

Table 1
Constants of the inclusion equilibrium of a dicarboxylate anion $^{-}OOC(CH_2)_n COO^{-}$ into the $[Cu_2^{II}(\mathbf{8})]^{4+}$ cryptate

n	log K	d(O···O) (Å)	Δd(O···O) (Å)
3	4.1	6.04	−1.32
4	6.9	7.20	−0.16
5	7.0	7.83	0.37
6	4.8	9.67	2.31

d(O···O) indicates the most convenient distance of the oxygen atoms of the two carboxylate groups, as obtained from crystal structures of the ammonium salts. Δd(O···O) is the difference between d(O···O) and 7.36 Å.

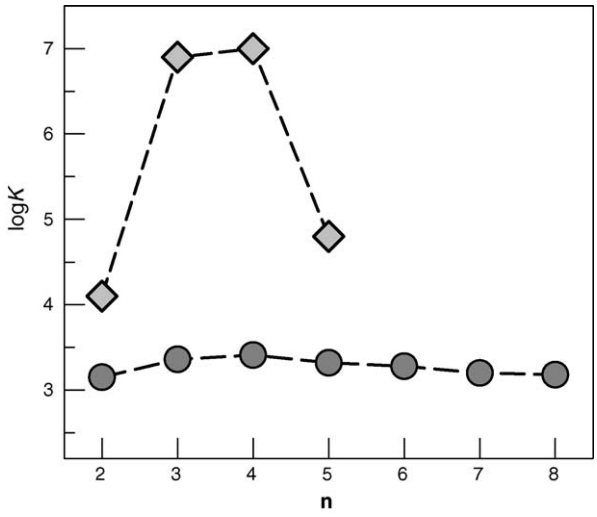

Fig. 14. Inclusion constants of aliphatic dicarboxylates ($^{-}$OOC–$(CH_2)_n$–COO^{-}) into the dicopper(II) cryptate $[Cu_2^{II}(\mathbf{8})]^{4+}$ (pH 7, diamonds) and into the hexaprotonated cryptand **21** (pH 6, circles).

tion is observed with respect to other anionic neurotransmitters and related amino acids. L-Aspartate (**25**) possesses two carboxylate groups like L-glutamate, but, due to the rather short distance between opposite oxygen atoms, forces the cryptate to an endoergonic rearrangement. γ-Amino butyrrate (GABA) and δ-amino pentanoate have only one carboxylate group: the amine group can act as a donor towards Cu^{II}, but its deprotonation is an energetically costly process. It may seem paradoxical that the β-amino acid glycine (**23**) displays some competitive behaviour: however, curve fitting studies indicated that two molecules of glycine are included within the cryptate. Double inclusion is not allowed to the γ- and δ-amino acids **26** and **27**, and also to the β-amino acid alanine (**24**), due to the increased steric hindrance (with respect to glycine).

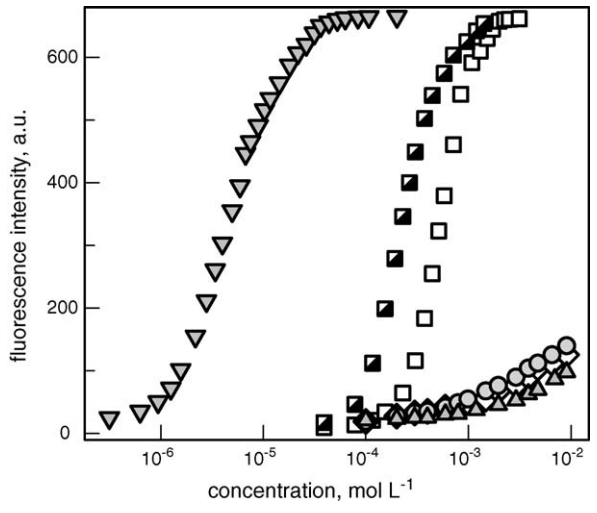

Fig. 15. Titration of a solution 2.5×10^{-6} M in $[Cu_2^{II}(\mathbf{8})]^{4+}$ and 2.5×10^{-7} M in **10** with glutamate and other neurotransmitters, in an aqueous solution buffered at pH 7. Triangles down: L-glutamate; half-filled squares: L-aspartate; squares: glycine; circles: δ-aminopentanoate; diamonds: γ-aminobutyrrate; triangles up: L-alanine. The fluorescence intensity of the indicator **10** is plotted vs. the logarithm of anion concentration.

2.4. A receptor containing three metallocyclam subunits, suitable for citrate recognition

A receptor for a tricarboxylate would require the presence within the cavity of *three* unsaturated transition metal centres. In this sense, we have appended three cyclam rings to the 1,3,5-trimethylbenzene platform, to give molecule **28** [31].

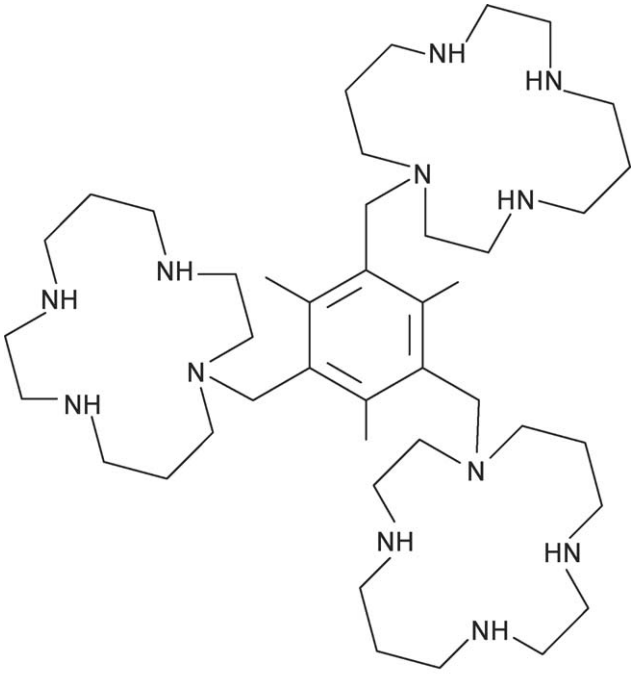

28

Cyclam typically incorporates transition metal ions to give very stable complexes from both a thermodynamic and a kinetic point of view [32]. Inertness is an important feature, when designing a metal containing receptor, as it prevents demetallation by the anionic substrate when present in excess. We prepared the tricopper(II) complex of **28** and we investigated its binding tendencies towards tricarboxylates and some competing anions in aqueous neutral solution [31].

The investigation was carried out following the indicator displacement paradigm. As a fluorescent indicator we chose 5-carboxy-fluorescein (**11**), which possesses two carboxylate groups and a phenolate oxygen atom, capable of interacting with the Cu^{II} centres of the trimetallic receptor $[Cu_3^{II}(\mathbf{28})]^{6+}$. **11** is strongly fluorescent in its anionic form, which is the dominating species in an aqueous solution adjusted to pH 7. When titrating a degassed solution of the indicator (5×10^{-7} M), buffered to pH 7 (HEPES 0.01 M), with a standard solution of $[Cu_3^{II}(\mathbf{28})]^{6+}$, complete quenching of the 5-carboxy-fluorescein emission was observed ($\lambda_{exc} = 450$ nm, $\lambda_{em} = 517$ nm). From the spectrofluorimetric titration profile, a binding constant of 5.78 ± 0.01 log units was calculated. Quenching is attributed to the occurrence of an intra-molecular electron or energy transfer process involving the photoexcited fluorescein subunit and the paramagnetic Cu^{II} centres of the receptor.

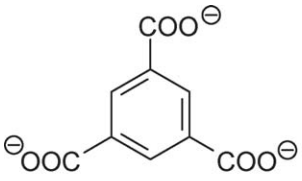

29

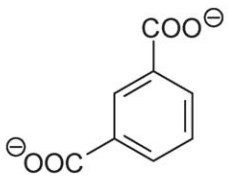

13

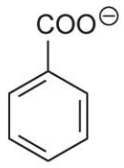

30

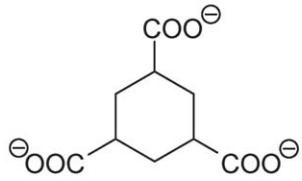

31

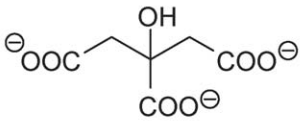

32

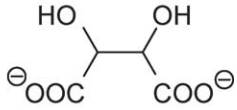

33

Then, an aqueous solution 2×10^{-5} M in $[Cu_3^{II}(\mathbf{28})]^{6+}$ and 5×10^{-7} M in **11**, buffered to pH 7, was titrated with standard solutions of some selected polycarboxylates. Titration profiles are shown in Fig. 16.

The anion 1,3,5-benzenetricarboxylate (**29**, $[C_6H_3(COO)_3]^{3-}$) fully displaces the indicator from the trimetallic receptor, giving rise to a rather steep profile, from which a $\log K = 5.81 \pm 0.01$ was calculated (equilibrium: $[Cu_3^{II}(\mathbf{28})]^{6+} + [C_6H_3(COO)_3]^{3-} \leftrightarrows [Cu_3^{II}(\mathbf{28})(C_6H_3(COO)_3]^{3+}$). Such a high value of the binding constant reflects the geometrical complementariety of the $[Cu_3^{II}(\mathbf{28})]^{6+}$ receptor and of the $[C_6H_3(COO)_3]^{3-}$ anion, both possessing a C_{3v} symmetry. In particular, the negatively charged oxygen atom of each carboxylate group should establish a coordinative interaction with the Cu^{II} centre of each metallocyclam subunit, which reaches five-coordination. The tendency of Cu^{II} complexes with cyclam derivatives (especially if having alkyl substituents on amine nitrogen atoms) is well known. A tentative sketch of the geometrical arrangement of the $[Cu_3^{II}(\mathbf{28})(C_6H_3(COO)_3]^{3+}$ supercomplex is illustrated in Fig. 17.

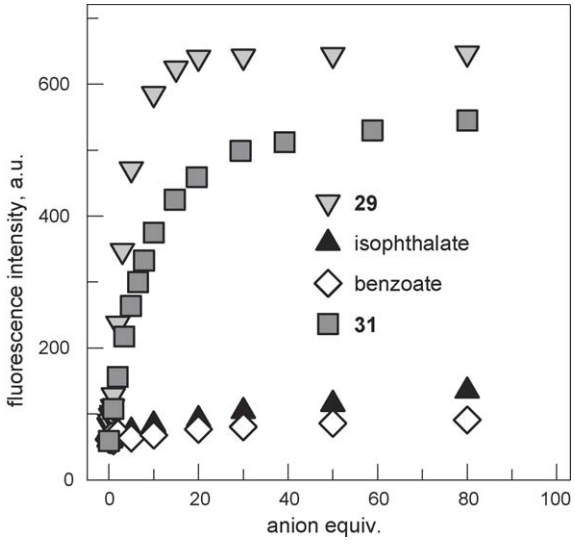

Fig. 16. Profiles obtained on titration of an aqueous solution 2×10^{-5} M in $[Cu^{II}_3(\mathbf{28})]^{6+}$ and 5×10^{-7} M in **11**, and buffered to pH 7 with HEPES (0.01 M) with selected polycarboxylates.

Noticeably, the bidentate anion 1,3-benzenedicarboxylate (isophthalate, **13**) and the monodentate benzoate (**30**) show smoother titration profiles (see Fig. 16), to which much smaller values of $\log K$ correspond (<3). The other tricarboxylate anion *cis*,*cis*-1,3,5-cyclohexanetricarboxylate (**31**), which possesses a C_{3v} symmetry, too, forms with $[Cu_3^{II}(\mathbf{28})]^{6+}$ a rather stable complex ($\log K = 5.00 \pm 0.01$), but less stable than the aromatic tricarboxylate **29** (notice the less steep titration profile in Fig. 16). The higher affinity displayed by **29** can be ascribed to the occurrence of an additional π–π interaction between the aromatic ring of the receptor platform and that of the anion **29**. Most interestingly, for analytical purposes, receptor $[Cu_3^{II}(\mathbf{28})]^{6+}$ forms a very stable 1:1 supercomplex with the tricationic anion citrate (**32**, $\log K = 5.59 \pm 0.01$), whose three carboxylate groups can coordinate the three Cu^{II} centres, in a similar way as **29**. Determination of citrate is important in the analytical control of beverages. In particular, receptor $[Cu_3^{II}(\mathbf{28})]^{6+}$ shows a neatly lower affinity with competing analytes like maleate ($\log K = 4.5 \pm 0.1$), tartrate ($\log K = 4.1 \pm 0.1$), succinate ($\log K = 3.8 \pm 0.1$), which all contain two carboxylate groups and cannot span the three Cu^{II} centres. Notably, the 1,3,5-trialkylbenzene scaffold had been previously functionalized with three arms containing guanidinium groups, to generate a tricationic receptor, which formed complex with the citrate anion in water with $\log K = 3.8$ [32]. Affinity toward citrate has been recently increased by appending to the same 1,3,5-trialkylbenzene platform three side chains containing the guanidiumcarbonyl pyrrole functionality, to give $\log K = 4.9$ at pH 7 [33]. The higher stability of the citrate complex with the sexicationic receptor $[Cu_3^{II}(\mathbf{28})]^{6+}$, in an aqueous solution buffered at neutral pH ($\log K = 5.59 \pm 0.01$) confirms the higher efficiency of metal containing systems as anion receptors in aqueous solution.

3. Anion recognition based on hydrogen bonding

3.1. Urea as a neutral receptor for anions

Most ligands of classical coordination chemistry are neutral (beginning from the first molecule deliberately used as a ligand: ammonia [34]). On the other hand, anion coordination chem-

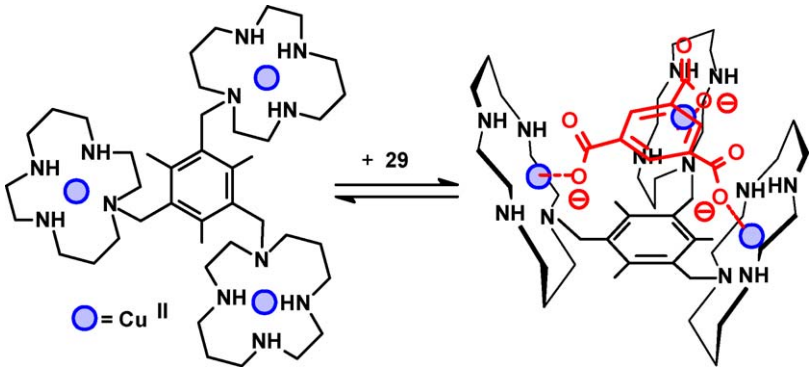

Fig. 17. Hypothesized geometric arrangement of the $[Cu_3^{II}(\mathbf{28})(C_6H_3(COO)_3)]^{3+}$ supercomplex. Figure reproduced from ref. [31], with permission of the copyright owners.

istry developed with the design of multi-point positively charged receptors, as mentioned in the Introduction [1,2]. Later, neutral receptors for anions came. The interaction a neutral receptor can establish with an anion is hydrogen bonding. In particular, the receptor must act as an H-bond donor and the anion as an H-bond acceptor. Suitable fragments for H-bond donation are –OH and –NH. Due to the higher electronegativity of oxygen, the O–H bond is more polarized, from which results that –OH is a more powerful H-bond donor than –NH. The unfortunate consequence is that water cannot be used as a medium for recognition studies based on hydrogen bonding. Thus, artificial neutral receptors typically contain one or more –NH fragments and their interactions with anions must be investigated in aprotic solvents like $CHCl_3$, MeCN, DMSO.

One of the most classical and first investigated –NH containing receptors was urea [13]. Urea and its derivatives are able to donate two hydrogen bonds to Y^- shaped anions such as acetate, to give an H-bond complex, whose hypothesized structure is shown in Scheme 2.

After the pioneering papers by Wilcox and co-workers [35], and Hamilton and co-workers [36], a variety of receptors containing one or more urea subunits have been designed and tested for anion recognition and sensing over the past decade. Recently, the crystal and molecular structure of complex **34** has been reported (see Fig. 18), which emphasizes the directionality of the bifurcate hydrogen bonding interaction with the acetate ion [37].

Acetate establishes two directional H-bonds with the two –NH fragments of the urea subunit. The N(urea)–O(acetate) distances (2.69 and 2.77 Å) position the interaction among 'moderate' hydrogen bonds, whose nature is mainly electrostatic [38]. The interaction of receptor **34** with CH_3COO^- was investigated in the aprotic solvent MeCN, through spectrophotometric titration experiments [37]. Fig. 19 shows the family of spectra taken over the course of the titration.

On addition of CH_3COO^-, the band at 345 nm progressively decreases, while a new band at 370 nm forms and develops. The well defined red-shift of the charge transfer band is ascribed to the fact that, on interaction with the acetate ion, electron density is transferred on the urea moiety, which makes the intensity of the dipole increase and shifts the charge transfer band to a longer wavelength. The presence of two sharp

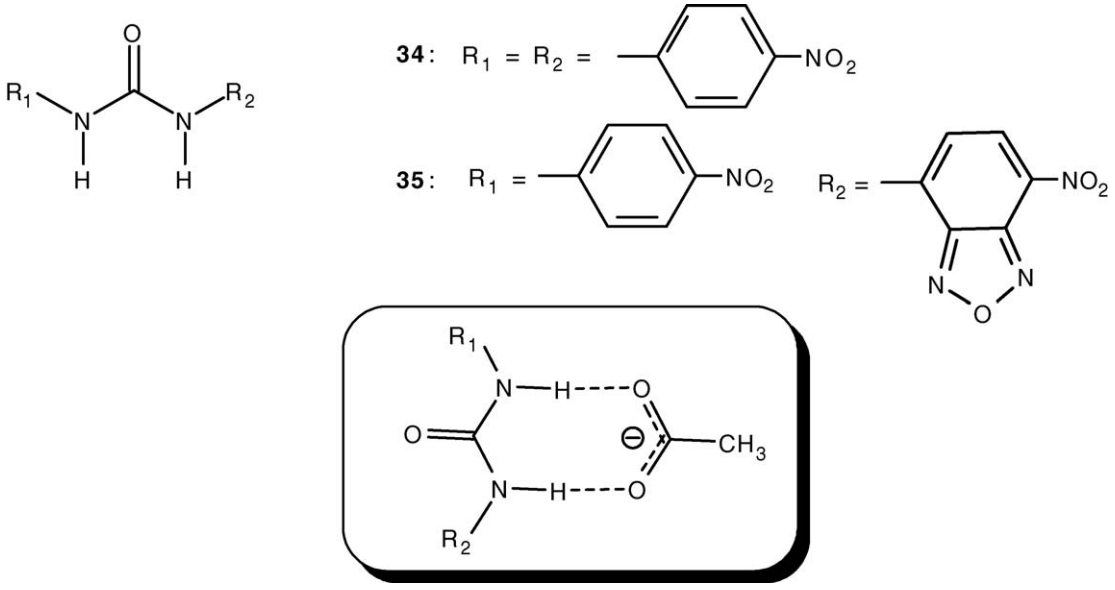

Scheme 2. The H-bond complex between a urea based receptor and acetate. The structure emphasises the directionality of the hydrogen bonding interaction.

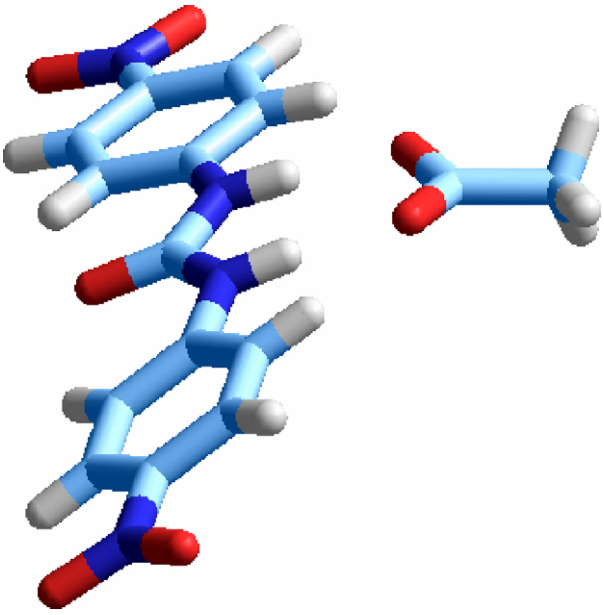

Fig. 18. The molecular structure of the H-bond complex of the urea based receptor **34** with acetate. The countercation tetrabutylammonium has been omitted for clarity.

isosbestic points indicates that only two species co-exist according to the equilibrium: $L + CH_3COO^- \leftrightarrows [L\cdots CH_3COO]^-$, in which $[L\cdots CH_3COO]^-$ represents the receptor–anion complex, whose structural features are illustrated in Scheme 2 and in Fig. 18. On non-linear fitting of titration profile, the binding constant was calculated: $\log K = 6.61 \pm 0.01$.

Analogous investigations were carried out with a variety of oxoanions ($H_2PO_4^-$, NO_3^-, NO_2^-, HSO_4^-, $C_6H_5COO^-$). In all cases, a new absorption band at ca. 370 nm developed on titration and sharp isosbestic points were observed in the recorded family of spectra. $\log K$ values for all investigated oxoanions are reported in Table 2.

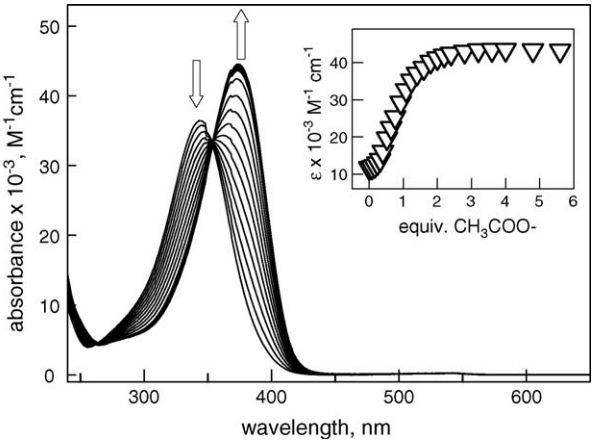

Fig. 19. Spectra taken over the course of the titration of a solution 2.6×10^{-5} M in **34** with a standard solution of $[Bu_4N]CH_3COO$, at 25 °C. *Inset*: Titration profile for a solution 1.0×10^{-6} M in **34**, from which the association constant was determined, $\log K = 6.61 \pm 0.09$. During the titration, the colour of the solution turns from pale yellow to bright yellow.

Table 2
Constants of the complex formation equilibrium, in an MeCN solution at 25 °C: **34** + anion$^- \leftrightarrows$ [**34**···anion]$^-$

anion	log *K*
CH_3COO^-	6.61 ± 0.01
$C_6H_5COO^-$	6.42 ± 0.01
$H_2PO_4^-$	5.37 ± 0.01
NO_2^-	4.33 ± 0.01
HSO_4^-	4.26 ± 0.01
NO_3^-	3.65 ± 0.05

The sequence of the $\log K$ values ($CH_3COO^- > C_6H_5COO^- > H_2PO_4^- > NO_2^- > HSO_4^- > NO_3^-$) seems to reflect the decreasing intrinsic basicity of the anion. In particular, a reasonably linear correlation was observed between $\log K$ and the average negative charge on the oxygen atoms of each oxoanion, as calculated through an ab initio method (see Fig. 20).

The higher the negative charge, the higher the H-bond acceptor tendencies of the anion. It has been recently pointed out that: "all hydrogen bonds can be considered as incipient proton transfer reactions, and for strong hydrogen bonds, this reaction can be in a very advanced state" [39].

The linear relationship in Fig. 20 provides a nice experimental evidence of the above statement. In fact, the partial negative charge on oxygen atoms gives a direct measure of the intrinsic basicity of the oxoanion. The stronger the basicity, the more pronounced the transfer of the –NH hydrogen toward the oxygen. The situation is pictorially illustrated in Fig. 21.

Following the interaction with the oxoanion, the urea H atom moves toward the oxygen atom of the anion along the N to O straight-line. The higher the partial negative charge on the oxygen atom (i.e, the higher anion basicity), the more pronounced the displacement of the H atom along each N to O line and the higher the energy of the hydrogen bonding interaction.

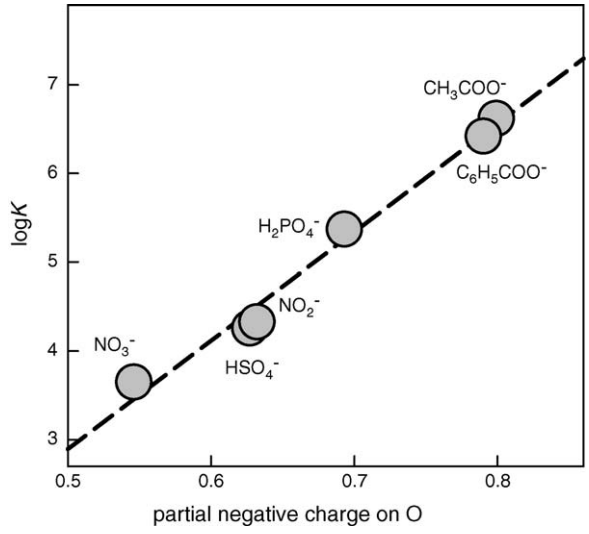

Fig. 20. A linear relationship between the log *K* value of the complexation equilibrium: **34** + $X^- \leftrightarrows$ [**34**···X]$^-$ in MeCN and the average partial negative charge on the oxygen atom of the oxoanion X^-. Partial charges were calculated through an ab initio method.

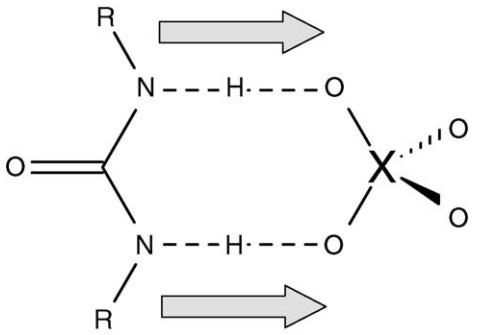

Fig. 21. The hydrogen bonding interaction viewed as the transfer of the protons from urea nitrogen atoms to the oxygen atoms of the oxoanion. The higher the partial negative charge on the oxygen atoms, the more pronounced the displacement of the hydrogen atoms from N to O and the higher the energy of the hydrogen bonding interaction.

3.2. The nature of urea–fluoride interaction

On these premises, one should anticipate that in a limiting situation, i.e. in the presence of a particularly basic anion X^-, a neat and definitive proton transfer process should take place, with deprotonation of one –N–H fragment of the urea subunit and formation of HX (according to a classic Brønsted acid–base equilibrium). Such a circumstance is not hypothetical, but has been observed in the case of fluoride.

Fig. 22 shows the complete family of spectra obtained during the titration of an MeCN solution 1.0×10^{-6} M in **34** with $[Bu_4N]F$ [37]. In the first part of the titration, the behaviour is similar to that observed for acetate and other investigated oxoanions: the colour of the solution changes from pale yellow to intense yellow, while, in the absorption spectrum, the band at 345 nm decreases and a band at 370 nm forms and develops. In particular, the band at 370 nm reaches its limiting value after the addition of 1 equiv. of fluoride. However, something new occurs on addition of the second equivalent of fluoride: the solution takes a red colour and a new band forms at a much higher wavelength: 475 nm, to reach a limiting value after the addition of 5 equiv. of F^-. The titration profiles shown in the insets (a and b) clearly indicate the presence of two well distinct steps.

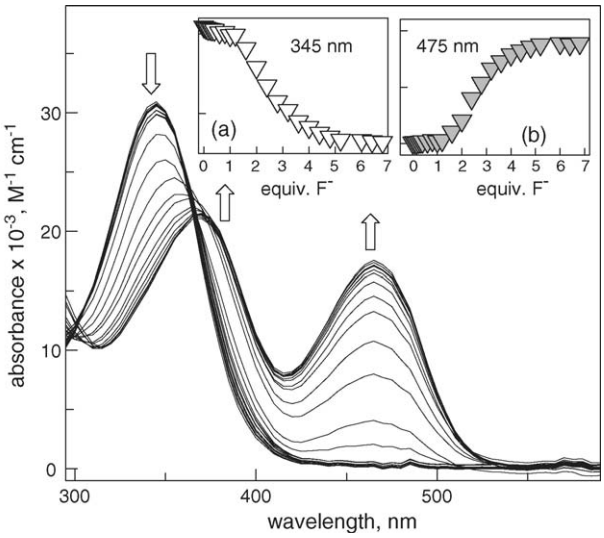

Fig. 22. Spectra taken over the course of the titration of an MeCN solution 1.0×10^{-6} M in **34** with a standard solution of $[Bu_4N]F$, at 25 °C. *Inset a*: Titration profiles of the band at 345 nm, which monitor the formation the H-bond complex $[\mathbf{34}^{\bullet}F]^-$. *Inset b*: Titration of the band at 475 nm, which monitors the formation of deprotonated form of **34**.

It is suggested that, in the first step, the formation of the H-bond complex takes place, as described by Eq. (4), in which LH represents the urea derivative **34** and X = F.

$$LH + X^- \leftrightarrows [LH \cdot X]^- \quad (4)$$

$$[LH \cdot X]^- + X^- \leftrightarrows L^- + [HX_2]^- \quad (5)$$

Then, on further addition of F^-, one HF molecule is removed from the complex to form the hydrogendifluoride ion, $[HF_2]^-$, while the urea receptor remains deprotonated, see Eq. (5). The following stepwise constants were calculated for the two consecutive equilibria: $\log K_1 = 7.38 \pm 0.09$ and $\log K_2 = 6.37 \pm 0.12$. Thus, the band at 475 nm must correspond to the deprotonated urea.

On the other hand, on titration of an MeCN solution of **34** with $[Bu_4N]Cl$, an absorption band developed at 370 nm, as observed for previously mentioned oxoanions. No band development at higher wavelengths was detected also on addition of a large excess of chloride. Thus, in the case of chloride, the typical H-bond complex $[\mathbf{34}\cdots Cl]^-$ is formed, whose binding constant was calculated from the titration profile: $\log K = 4.55 \pm 0.01$.

Thus, the fluoride ion displays a distinctive behaviour, inducing deprotonation of one of the –NH fragments. This seems to be due to the unique stability of the $[HF_2]^-$ self-complex, for which the highest hydrogen bond energy in the gas phase has been calculated (39 kcal mol^{-1}) [40]. Thus, if *one* F^- ion is a fairly strong base in an MeCN solution, as documented by its ability to form with **34** a stable H-bond complex, *two* F^- ions represent a very strong base, being capable to induce deprotonation of urea. The acidity of the urea moiety has been strongly enhanced due to the presence of two electron-withdrawing nitro substituents on the covalently linked phenyl rings. Fluoride induced deprotonation of one –NH fragment has been unambiguously demonstrated also through ^1H NMR titration experiments [37].

However, the most convincing evidence of the formation of a new and unexpected species typically comes from its crystal and molecular structure. This was not observed with receptor **34**, but with the similar system **35**, in which a nitrophenyl substituent has been replaced by a nitrobenzofurazan subunit [41]. Also in the present case, on fluoride addition, the pale yellow solution of **35** in MeCN became intensely red, and titration data indicated the occurrence of the two consecutive equilibria: (i) formation of a genuine H-bond complex, and (ii) –N–H deprotonation and formation of the $[HF_2]^-$ self-complex. Most interestingly, on diffusion of diethylether on an MeCN solution containing **35** (LH) and excess of tetrabutylammonium fluoride, crystals of a salt of formula $[Bu_4N]L$ were obtained, suitable for X-ray diffraction studies. Fig. 23 reports the molecular structure of the salt [41].

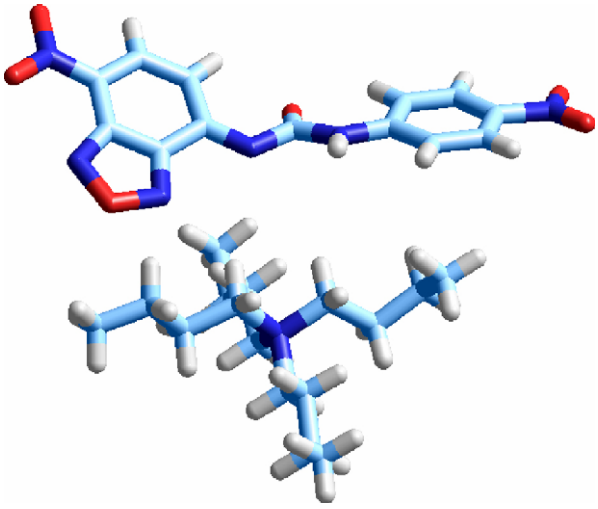

Fig. 23. The molecular structure of the $[Bu_4N]L$ salt (L = **35**). The –NH fragment close to the more electron-withdrawing nitrobenzofurazan moiety underwent deprotonation.

Deprotonation has taken place at the –N–H fragment close to the more electron-withdrawing nitrobenzofurazan subunit. Deprotonation induces significant structural modifications in the framework of the urea derivative **35**. The 1,3-diphenyl substituted urea molecules, e.g. that present in the H-bond complex shown in Fig. 18, are almost completely flat, the two phenyl rings and the –HN(CO)NH– fragment lying in the same plane, in the absence of steric effects between adjacent molecules. In contrast, in the L^- anion shown in Fig. 23, the benzofurazan group forms a dihedral angle of 42.4°, with the plane containing the nitrophenyl urea subunit. It is suggested that, following –NH deprotonation, a significant electronic rearrangement takes places, as illustrated by the π-resonance representation in Scheme 3.

In fact, the distance between the deprotonated nitrogen and the carbon atom of the nitrobenzo-furazan subunit (1.317 Å) is noticeably shorter than that between the other nitrogen atom and the carbon atom of the nitrophenyl substituent (1.393 Å). Moreover, significant differences are observed also in the two nitro groups: that linked to the benzofurazan moiety present a shorter C–N distance (1.38 Å) and a longer N–O distance (1.25 Å), than that linked to the phenyl ring (1.39 and 1.21 Å, respectively). This suggests the occurrence, on deprotonation, of a delocalization of the negative charge of nitrogen towards the nitrobenzofurazan moiety and that the deprotonated system L^- is better represented by the resonance formula **b** in Scheme 3. Thus, on deprotonation, the phenyl ring of the nitrobenzofurazan subunit loses in part its aromaticity and is therefore excluded from the extended π-system responsible for diphenylurea coplanarity. As a consequence, the benzofuran moiety can undergo a rotation of 42.4°, probably in order to minimise steric repulsions with the carbonyl oxygen atom.

3.3. Urea versus thiourea

We have pointed out that (i) the hydrogen bonding interaction can be conveniently considered as an incipient and 'frozen' proton transfer from the donor B–H (e.g. urea) to the acceptor A^- (e.g. an anion), along an ideal B···H···A straight-line; (ii) the more pronounced the proton transfer, the stronger the hydrogen bonding interaction (and the higher the solution stability of the H-bond complex that forms). Then, in the realm of anion recognition, the most stable H-bonded complexes will be formed by more basic anions (along the series: $CH_3COO^- > C_6H_5COO^- > H_2PO_4^- > NO_2^- > HSO_4^- > NO_3^-$) and by more acidic receptors. The latter feature explains why most urea based receptors contain electron-withdrawing substituents (e.g. 4-nitrophenyl), which, as push–pull chromophores, also provide a useful signalling mechanism.

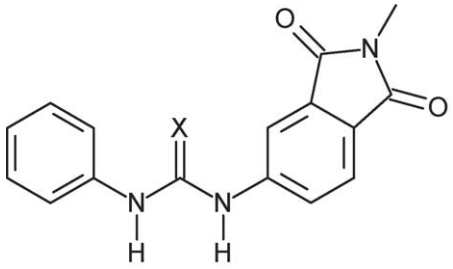

There exists another way to increase the acidity of the receptor: replacing the urea fragment with a thiourea fragment. In fact, in a DMSO solution, thiourea ($pK_A = 21.1$) is a much stronger Brønsted acid than urea ($pK_A = 26.9$) [42]. In order to verify such an effect, we considered molecules **36** and **37** as anion receptors in DMSO solution [43]. In the two derivatives, a phthalimide substituent, a classical chromophore, has been appended at one nitrogen atom of the urea/thiourea subunit, in order to provide an optical signal for reporting on the receptor–anion interaction.

The urea derivative **36** showed the same behaviour observed with **34** and **35**: CH_3COO^-, $C_6H_5COO^-$, $H_2PO_4^-$ and Cl^- formed 1:1 H-bond complexes, as represented by Eq. (4), whose equilibrium constants are reported in Table 3. On the other hand, F^- formed a genuine H-bond complex, Eq. (4) which, on further anion addition, underwent HF release with formation of the

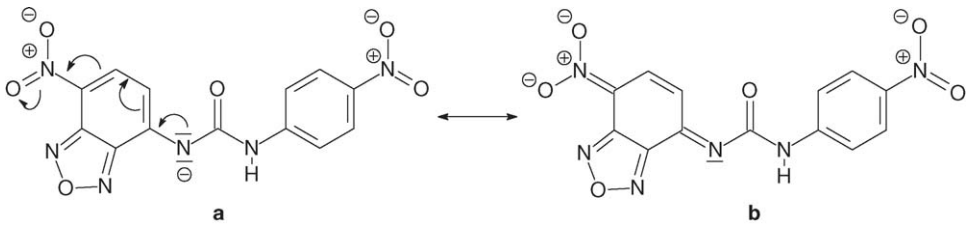

Scheme 3. A resonance representation of the deprotonated form of **35**.

Table 3
log K values for the interaction of receptors **36** (urea based) and **37** (thiourea based) with anions in DMSO solution at 25 °C

LH	Equilibrium	F^-	CH_3COO^-	$C_6H_5COO^-$	$H_2PO_4^-$	Cl^-
32	$LH + X^- \leftrightarrows [LH\cdots X]^-$	3.86 ± 0.05	4.63 ± 0.03	4.18 ± 0.01	4.47 ± 0.01	4.38 ± 0.01
	$[LH\cdots X]^- + X^- \leftrightarrows L^- + [HX_2]^-$	1.83 ± 0.11	–	–	–	–
33	$LH + X^- \leftrightarrows [LH\cdots X]^-$	5.7 ± 0.01	6.02 ± 0.05	5.77 ± 0.05	5.44 ± 0.06	4.88 ± 0.01
	$[LH\cdots X]^- + X^- \leftrightarrows L^- + [HX_2]^-$	5.5 ± 0.3	3.23 ± 0.10	3.36 ± 0.10	0.55 ± 0.11	–

$[HF_2]^-$ self-complex and of the deprotonated receptor L^-, see Eq. (5).

Equally, the thiourea containing receptor **37** forms 1:1 authentic H-bonded complexes with all the anions investigated. However, *all* complexes, except that with chloride, on excess addition of anion, release an HX molecule, to give L^- and the self-complex $[HX_2]^-$. As an example, the proposed structure of the $[HX_2]^-$, in the case of $X^- = CH_3COO^-$ is sketched below:

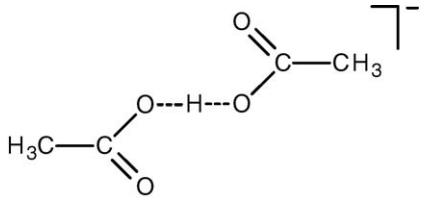

In order to explain the different behaviour of the two receptors, it is convenient to consider equilibrium (6), which results from the sum of Eqs. (4) and (5):

$$LH + 2X^- \leftrightarrows L^- + [HX_2]^- \quad (6)$$

The constant of Eq. (6) is $\beta_2 = K_A(LH) \times \beta([HX_2]^-)$, where $K_A = [L^-] \times [H^+]/[LH]$ and $\beta([HX_2]^-) = [HX_2]^-/[H^+] \times [X^-]^2$. Receptor **36**, which contains the less acidic urea subunit, undergoes deprotonation and HF release only in the presence of F^-, in view of the extremely high stability of $[HF_2]^-$ and high value of the formation constant $\beta([HX_2]^-)$. In the case of the thiourea containing receptor **37**, in view of its remarkably higher acidity (high value of K_A), deprotonation can take place in the presence of a greater number of anions. In particular, the value of β_2 decreases with the decreasing stability of the self-complex $[HX_2]^-$: $F^- > CH_3COO^- \sim C_6H_5COO^- > H_2PO_4^-$. In the case of dihydrogenphosphate, due to the rather low stability of the $[(H_2PO_4)\cdots(H_3PO_4)]^-$ self-complex, significant –N–H deprotonation is observed only after the addition of several equivalents of $[Bu_4N]H_2PO_4$. Fig. 24 displays the family of spectra obtained over the course of the titration. The shoulder at 410 nm, pertinent to the deprotonated receptor L^-, begins to develop after the addition of the second equivalent of the anion. The inset of Fig. 24 shows how the relative concentration of uncomplexed receptor LH, the H-bonded complex $[LH\cdots H_2PO_4]^-$ and the deprotonated form L^- vary over the course of the titration. The $[LH\cdots H_2PO_4]^-$ complex reaches its maximum concentration with the addition of 1 equiv. of dihydrogen phosphate. Then, on further anion addition, the complex begins to release H_3PO_4, which interacts with $H_2PO_4^-$ to give the self-complex $[H_3PO_4\cdots H_2PO_4]^-$. After the addition of 4 equiv., the deprotonated form has reached the relative concentration of only 30%.

Among the anions investigated, only chloride fails to induce the deprotonation of receptor **37**. In particular, the H-bond complex that forms, $[LH\cdots Cl]^-$, definitively resists the addition of a large excess of chloride, due to the poor stability of the $[HCl_2]^-$ self-complex.

The different behaviour of the two receptors is visually illustrated by the diagram reported in Fig. 25, in which the scale of $pK_A(LH)$ and that of $\log \beta([HX_2]^-)$ are tentatively juxtaposed. The diagram emphasises the concurrent contribution of (i) the intrinsic acidity of LH and (ii) the stability of $[HX_2]^-$ in inducing deprotonation: the receptor LH, either **36** or **37**, undergoes deprotonation in presence of those anions whose $\log \beta([HX_2]^-)$ values are placed above the pertinent horizontal line: solid for **36**, dashed for **37**.

3.4. Metal induced enhancement of H-bond donor tendencies of urea

Metal ions, in the appropriate geometrical circumstances, can improve the affinity of urea/thiourea based receptors toward anions. We have observed this effect on investigating system **38**, in which an NS_2O_2 crown has been covalently linked to a urea subunit. On the other side, a nitrophenyl group was appended, as a chromogenic reporter [44].

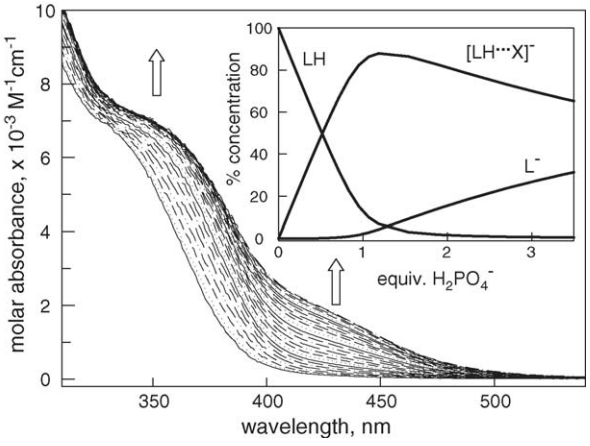

Fig. 24. Spectra taken over the course of the titration of a DMSO solution of **37** (5×10^{-6} M) with a standard solution of $[Bu_4N]H_2PO_4$. *Inset*: Change of the relative concentration of the species at equilibrium on phosphate addition (LH = **37**, $X^- = H_2PO_4^-$).

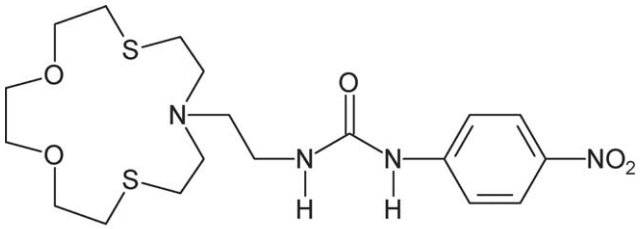

38

The crown ligand, due to the presence of the two thioethereal sulphur atoms, is expected to form stable complexes with d^{10} metal centres (soft). In particular, the complex of Cd^{II} with the NO_2S_2 macrocycle has been crystallographically characterized and showed full coordination of all the five donor atoms to the metal [45]. In our study, we considered a monopositively charged cation, in order to match the negative charge of the anion supposed to interact with the urea moiety, and we chose silver(I). Thus, titration experiments were carried out on adding the tetrabutylammonium salt of the envisaged anion on an MeCN solution of the receptor containing or not 1 equiv. of $AgNO_3$. Fig. 26 shows the spectra taken over the course of the titration with $[Bu_4N]CH_3COO$ of a solution of the urea based receptor **38**, in absence (Fig. 26a) and in presence of $AgNO_3$ (Fig. 26b).

In both experiments, on acetate addition, the charge transfer band of the receptor underwent a distinct red-shift. However, the titration profiles, shown in the inset, are remarkably different, whether in absence or in the presence of $AgNO_3$. The profile obtained in absence of metal (inset of Fig. 26a), shows a smooth curvature, to which an association constant of $\log K = 4.49 \pm 0.01$ corresponds. On the other hand, the titration profile in presence of equimolar Ag^I (inset of Fig. 26b) is much steeper and indicates that the association constant, in the circumstances investigated, must be higher than 10^6. Thus, the metal centre increases the anion affinity of the urea subunit more than 30 times.

The enhancement of anion affinity of the urea fragment is ascribed to the process pictorially illustrated in Scheme 4: interaction with acetate induces a transfer of negative charge to the oxygen atom of the carbonyl group, which therefore increases its donor tendencies and, following the movement of the pendant arm, goes to coordinate the proximate Ag^I centre. Metal binding

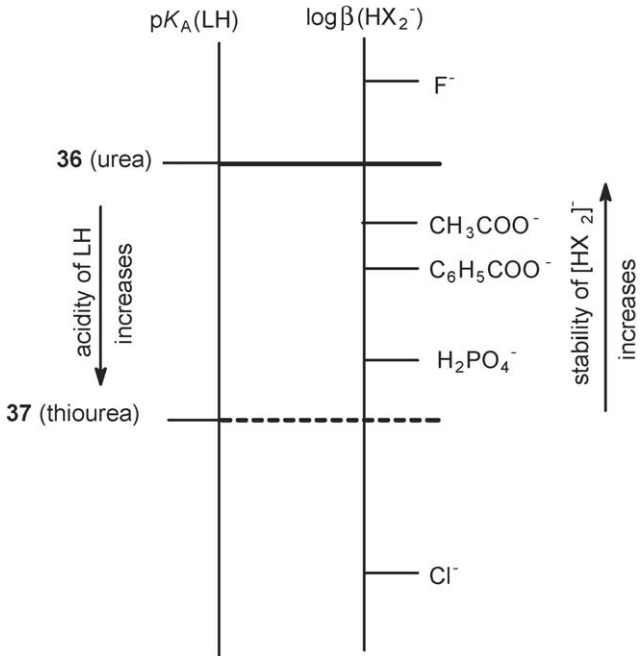

Fig. 25. Empirical juxtaposition of the acidity scale of the receptor LH (**36** and **37**, left vertical line) and of the stability scale of $[HX_2]^-$ (right vertical line). Each receptor deprotonates in presence of excess of anions whose log $\beta([HX_2]^-)$ values lie above the pertinent horizontal line: solid for **36**, dashed for **37**.

increases the polarization of the –N–H fragments and ultimately causes an increase of the hydrogen bonding interaction. Similar spectroscopic patterns were observed on performing titration experiments with $H_2PO_4^-$ and HSO_4^-. In both cases, an enhancement of anion affinity was observed, by a factor of 10 and 4, respectively (see values in Table 4).

However, the constants reported in Table 4 do not express the real affinity of the oxoanion toward the urea fragment of the Ag^I**/38** complex. In fact, titration experiments were carried out by using $AgNO_3$ as source of silver(I): thus, the nitrate ion was present in equimolar amount with respect to **38** and NO_3^- shows a definite affinity toward the Ag^I**/38** complex. This was demonstrated by the fact that, on titration with $[Bu_4N]NO_3$ of a solution containing both **38** and $Ag(CF_3SO_3)$, a distinct red-shift of the charge transfer band was observed and the corresponding asso-

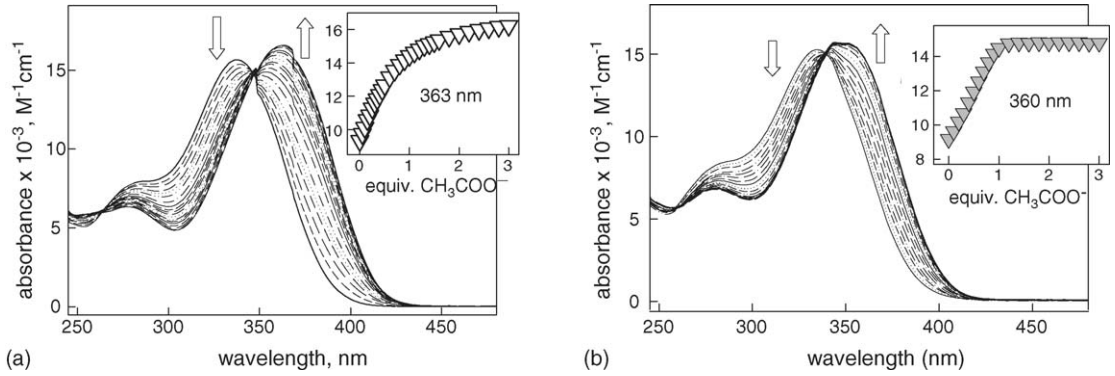

Fig. 26. Spectra taken over the course of the titration: (a) of an MeCN solution 1.0×10^{-4} M in **38** with a standard solution of $[Bu_4N]CH_3COO$; (b) of an MeCN solution 1.0×10^{-4} M both in **38** and in $AgNO_3$ with a standard solution of $[Bu_4N]CH_3COO$. *Inset*: Titration profiles at selected wavelengths.

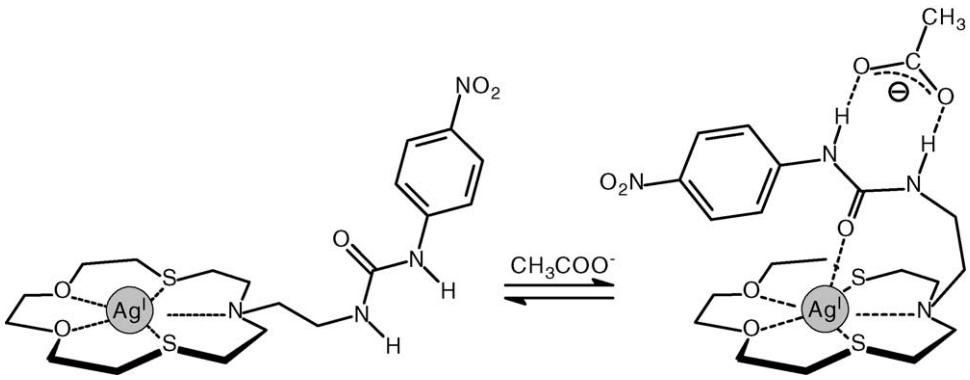

Scheme 4. Enhanced affinity of the urea subunit toward acetate, through coordination of the carbonyl oxygen atom to the proximate Ag^I centre.

Table 4
Equilibrium constants for the interaction of **38**, in the absence or in the presence of $AgNO_3$, with anions, in an MeCN solution, at 25 °C

Anion	**38**	**38** + $AgNO_3$	
	$\log K_1$	$\log K_1$	$\log K_2$
CH_3COO^-	4.49 ± 0.01	>6	–
$H_2PO_4^-$	3.72 ± 0.01	4.71 ± 0.01	–
HSO_4^-	3.18 ± 0.01	3.58 ± 0.01	–
F^-	4.05 ± 1	>6	>6

$\log K_1$ refers to the formation of a genuine H-bond complex $LH + X^- \leftrightarrows [LH\cdots X]^-$; $\log K_2$ refers to the deprotonation equilibrium: $[LH\cdots X]^- + X^- \leftrightarrows L^- + HX_2^-$ (LH = **38**; X^- = anion).

ciation constant ($\log K = 2.91 \pm 0.01$) was calculated. Thus, the constants reported in Table 4 do not correspond to an authentic association equilibrium, but rather to a process in which a nitrate ion is displaced from the receptor by the investigated anion. Absolute association constants are obtained by adding 2.9 to the $\log K$ values of Table 4. However, the presence of nitrate was essential in order to obtain smooth titration profiles and computable $\log K$ values. In fact, on using $Ag(CF_3SO_3)$ as silver(I) source, one would obtain profiles with a sharp bending at the equivalent point, on titration with any anion, thus being in the position to assess only the lower limit of 6 for $\log K$ values. Notice also that, in the absence of Ag^I, nitrate addition, even in large excess, did not induce any modification of the charge transfer band, indicating poor or nil affinity of NO_3^- toward the metal-free urea subunit, in the conditions investigated.

Quite predictably fluoride displayed unusual behaviour. Fig. 27a shows the spectra taken during the titration of an MeCN solution of **38** (10^{-4} M) with $[Bu_4N]F$. The typical red-shift of the charge transfer band was observed and the titration profile (see the diagram in the inset) indicated the formation of a stable H-bond, with an association constant $\log K = 4.01 \pm 0.01$. However, on titration of the solution containing equimolar $AgNO_3$, something more was observed (see Fig. 27b). The typical red-shift of the band at 332 nm and the steep titration profile (filled triangles in the inset) clearly indicate the formation of a very stable H-bond complex of 1:1 stoichiometry, with $\log K > 6$. However, a new band formed at 450 nm, which reached a *plateau* after the addition of 2 equiv. of fluoride (open circles in the inset). Appearance of the band at long wavelengths reveals the occurrence of the anion-induced deprotonation of one of the –N–H fragments of the urea subunit. Thus, the following two stepwise equilibria take place over the course of the titration with fluoride:

$$[Ag^+]LH + F^- \leftrightarrows [Ag^+][LH\cdots F]^- \quad (7)$$

$$[Ag^+][LH\cdots F]^- + F^- \leftrightarrows [Ag^+]L^- + [HF_2]^- \quad (8)$$

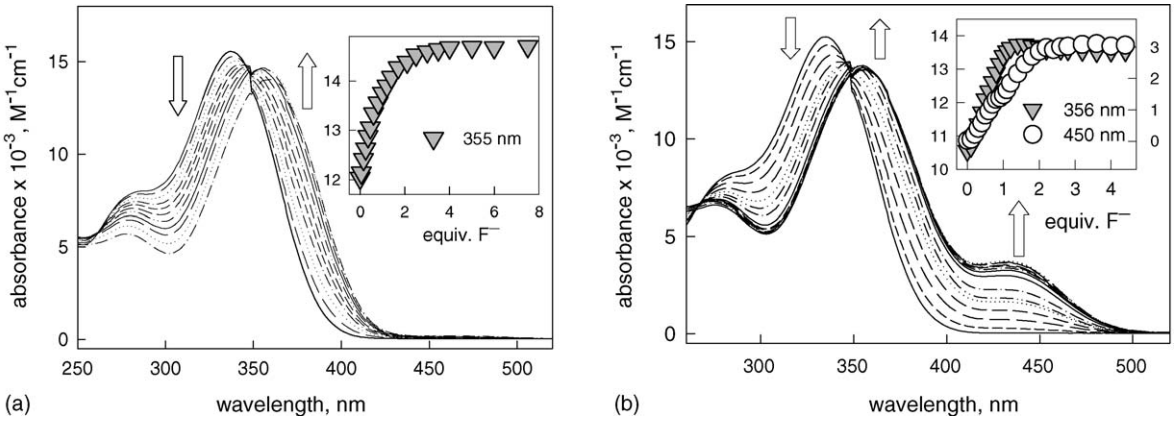

Fig. 27. Spectra taken during the titration: (a) of an MeCN solution 1.0×10^{-4} M in **38** with a standard solution of $[Bu_4N]F$; (b) of an MeCN solution 1.0×10^{-4} M in **38** and in $AgNO_3$ with a standard solution of $[Bu_4N]F$. *Inset*: Titration profiles at selected wavelengths (inset in (b): left vertical axis: molar absorbance of the band at 356 nm $\times 10^{-3}$; right vertical axis: molar absorbance of the band at 450 nm $\times 10^{-3}$.

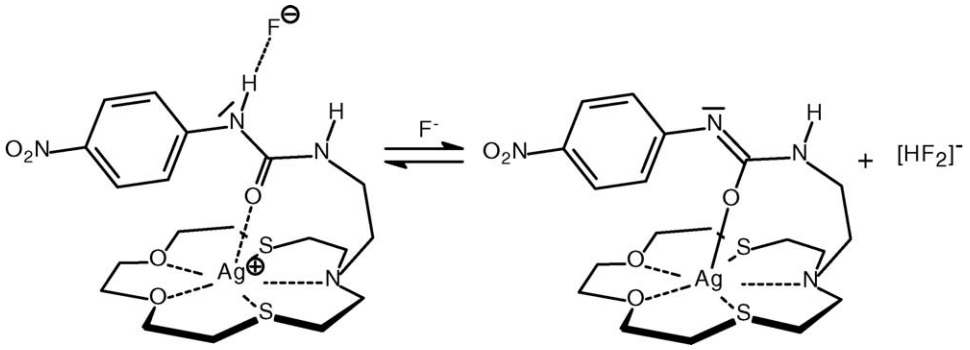

Scheme 5. Fluoride induced deprotonation of the urea subunit in the Ag^{I}/**38** complex.

where LH = **38**. In particular, the second F^- ion removes an HF molecule from $[Ag^+][LH\cdots F]^-$ to give the H-bond self-complex $[HF_2]^-$. Such a process is favoured by the extreme stability of the $[HF_2]^-$ self-complex, as outlined in previous sections. However, –N–H deprotonation does not take place with the metal-free receptor **38**. The role of Ag^I is essential, as, on interaction with the coordinating carbonyl oxygen atom, it strongly enhances the acidity of the –N–H groups.

The process is sketched in Scheme 5. In the Scheme, it is considered that, following –N–H deprotonation, electron density is transferred, through a π conjugative mechanism, from the nitrogen atom to the oxygen atom, which changes from an sp^2 to an sp^3 hybridization, and finally to the metal centre (which reduces its electrical charge from 1+ to 0).

System **38** can be rightfully considered an ion-pair receptor, i.e. a ditopic ligand capable of simultaneous complexation of a metal ion and an anion [46]. Binding of the two ions can occur independently, or, more interestingly, can profit from cooperative effects. For instance, Smith has recently designed polycyclic receptors containing amide –N–H fragments, capable of accomodating a cation (e.g. K^+) and an anion (e.g. Cl^-) in close contact [47]: in the presence of K^+, the receptor's affinity toward Cl^-, in a DMSO solution, was 13-fold enhanced, due to a cooperative electrostatic effect. In system **38**, a dramatically favourable cooperative effect, of more complicated nature, is observed; for instance, affinity of the urea subunit toward CH_3COO^-, in the presence of Ag^I, increases by more than four orders of magnitude.

4. Moral of the story

We have reviewed some work on anion recognition and sensing carried out in this Laboratory during the past years and we would like to comment on the general principles for the design of ideal receptors for chosen anions. Metal–ligand interactions are relatively strong and in most cases more than compensate the endoergonic terms associated to anion desolvation. As a consequence, receptors containing transition metal ions ensure selective anion recognition in pure water, at pH 7. Copper(II) is particularly recommended as a metal centre, because, among 3d divalent metal ions, it establishes the strongest coordination bonds with most donor atoms. Moreover, its intrinsic kinetic lability allows fast exchange of ligands, including anions, thus providing the basis for sensing activity. The Cu^{II} ion must preliminarily and firmly interact with a tetramine donor set and will tend to reach the preferred five-coordination through the interaction with a further ligand, possibly the investigated anion. The most often used tetramine platform is that of tren, which favours the formation of a complex of trigonal bipyramidal geometry (usually compressed), in which one axial position is reserved to the donor atom of the anion. A further platform is provided by the cyclic tetramine cyclam, whose Cu^{II} complex is naturally predisposed to five-coordination, according to a square pyramidal geometry (in which the donor atom of the anion goes to occupy the apical position). The metallocyclam scaffold provides an extra bonus, as the Cu^{II} centre, due to inertness imposed by the 14-membered cyclic tetramine (the kinetic macrocyclic effect) cannot be removed from the receptor, even in the presence of a large excess of anion. On the other hand, the lability of the apical position is maintained, which ensures fast and reversible sensing activity.

However, in spite of these relevant qualities, metal containing receptors are quite rare, and the attention of researchers in anion chemistry has been and is currently mainly devoted to purely organic receptors, in most cases neutral. Indeed, very sophisticated neutral receptors have been synthesized, whose cavity has been designed for the selective inclusion of anions of varying shape and size. The limit of neutral systems is that interactions they provide, e.g. hydrogen bonding, are not very strong and that, in any case, even the most efficient H-bond donating receptor cannot compete with water. This confines investigations to aprotic media, possibly not too polar. However, the receptor–anion interaction based on hydrogen bonding interaction is per se interesting, and this prompted us to investigate (or re-investigate) the behaviour of some simple systems based on one of the most classic H-bond donors: urea. We observed that the receptor–anion interaction can be conveniently viewed as a more or less advanced (and 'frozen') transfer of a proton from the –N–H fragment of urea to the binding atom of the anion. Thus, the selectivity is solely associated with the basic tendencies of the anion, whereas geometric features do not matter at all. For instance, modeling shows that the NO_3^- ion has its oxygen atoms at a proper distance to match the hydrogen atoms of urea derivatives. However, NO_3^- forms with urea based receptors much less stable complexes than $H_2PO_4^-$, which exhibits too large an O–O distance, but is distinctly more basic. Fluo-

ride is special as it forces the intra-complex proton transfer to the extreme limit: −N−H deprotonation. This is not due to the high basicity of F^- in aprotic solvent (which is lower than that of CH_3COO^-, for instance), but to the unique stability of the $[HF_2]^-$ self-complex. It is probably for this reason that most of the reported neutral anion receptors (having urea and amide binding sites) are proposed as selective sensors for fluoride. Most interestingly, recognition of fluoride is often signalled through the appearance of beautiful colours [48–59]. It should be now clear that colour development and drastic spectroscopic changes are associated with one-step, and sometimes two-step deprotonation of urea [60], which, more than as an H-bond donor, behaves as a Brønsted acid. In conclusion, urea based receptors can display geometrical rather than acid–base selectivity, only if the H-bond donor subunits are incorporated in a concave framework (possibly cyclic or polycyclic), providing strict steric constraints that overcome effects related to intrinsic acid–base properties.

Acknowledgments

The financial support by the European Union (RTN Contract HPRN-CT-2000-00029) and the Italian Ministry of University and Research (PRIN—Dispositivi Supramolecolari; FIRB—Project RBNE019H9K) is thankfully acknowledged. F.S. is grateful to the European Commission for an Intra-European 'Marie Curie' Fellowship (MEIF-CT-2003-500843).

References

[1] E. Graf, J.-M. Lehn, J. Am. Chem. Soc. 98 (1976) 6403.
[2] F.P. Schmidtchen, Angew. Chem. Int. Ed. Engl. 89 (1977) 751.
[3] B. Dietrich, J. Guilhem, J.-M. Lehn, C. Pascard, E. Sonveaux, Helv. Chim. Acta 67 (1984) 91.
[4] F.P. Schimdtchen, G. Müller, Chem. Commun. (1984) 1115.
[5] K. Bowman-James, Acc. Chem. Res. 38 (2005) 671.
[6] F.P. Schmidtchen, M. Berger, Chem. Rev. 97 (1997) 1609.
[7] A. Bianchi, K. Bowman-James, E. García-España (Eds.), Supramolecular Chemistry of Anions, Wiley-VCH, New York, 1997.
[8] L. Fabbrizzi, M. Licchelli, G. Rabaioli, A. Taglietti, Coord. Chem. Rev. 205 (2000) 85.
[9] P.D. Beer, P.A. Gale, Angew. Chem., Int. Ed. 40 (2001) 486.
[10] R. Martinez-Mañez, F. Sancenón, Chem. Rev. 103 (2003) 4419.
[11] C. Suksai, T. Tuntulani, Chem. Soc. Rev. 32 (2003) 192.
[12] P.A. Gale (Ed.), Coord. Chem. Rev. 240 (2003) 1.
[13] P.A. Gale, Amide- and Urea-Based Anion Receptors. Encyclopedia of Supramolecular Chemistry, Marcel Dekker, New York, 2004, p. 31.
[14] K. Choi, A.D. Hamilton, Encyclopedia of Supramolecular Chemistry, Marcel Dekker, New York, 2004, p. 566.
[15] J.M. Llinares, K. Bowman-James, Encyclopedia of Supramolecular Chemistry, Marcel Dekker, New York, 2004, p. 1170.
[16] A.P. Gale, J.L. Sessler, S. Camiolo, Encyclopedia of Supramolecular Chemistry, Marcel Dekker, New York, 2004, p. 1176.
[17] D. Chen, A.E. Martell, Tetrahedron 47 (1991) 6895.
[18] J.-M. Lehn, Acc. Chem. Res. 11 (1978) 49.
[19] C.J. Harding, F.E. Mabbs, E.J.L. MacInnes, V. McKee, J. Nelson, J. Chem. Soc., Dalton Trans. (1996) 3227.
[20] L. Fabbrizzi, P. Pallavicini, A. Perotti, L. Parodi, A. Taglietti, Inorg. Chim. Acta 238 (1995) 5.
[21] V. Amendola, E. Bastianello, L. Fabbrizzi, C. Mangano, P. Pallavicini, A. Perotti, A. Manotti Lanfredi, F. Ugozzoli, Angew. Chem., Int. Ed. Engl. 112 (2000) 3039.
[22] C.J. Harding, V. McKee, J. Nelson, Q. Lu, Chem. Commun. (1993) 1768.
[23] L. Fabbrizzi, A. Leone, A. Taglietti, Angew. Chem. Int. Ed. 40 (2001) 3066.
[24] S.L. Wiskur, H. Ait-Haddou, J.J. Lavigne, E.V. Anslyn, Acc. Chem. Res. 34 (2001) 963.
[25] L. Fabbrizzi, N. Marcotte, F. Stomeo, A. Taglietti, Angew. Chem. Int. Ed. 41 (2002) 3811.
[26] M. Ansa-Hortalá, L. Fabbrizzi, N. Marcotte, F. Stomeo, A. Taglietti, J. Am. Chem. Soc. 125 (2003) 20.
[27] L. Fabbrizzi, M. Licchelli, A. Taglietti, Dalton Trans. (2003) 3471.
[28] M. Boiocchi, M. Bonizzoni, L. Fabbrizzi, G. Piovani, A. Taglietti, Angew. Chem., Int. Ed. 43 (2004) 3847.
[29] J.-M. Lehn, R. Méric, J.-P. Vigneron, I. Bkouche-Waksman, C. Pascard, Chem. Commun. (1991) 62.
[30] M. Bonizzoni, L. Fabbrizzi, G. Piovani, A. Taglietti, Tetrahedron 60 (2004) 11159.
[31] L. Fabbrizzi, F. Foti, A. Taglietti, Org. Lett. 7 (2005) 2603.
[32] A. Metzger, E.V. Anslyn, Angew. Chem., Int. Ed. 37 (1998) 649.
[33] C. Schmuck, M. Schwegmann, J. Am. Chem. Soc. 127 (2005) 3373.
[34] A. Werner, Z. Anorg. Allg. 3 (1893) 267.
[35] P.J. Smith, M.V. Reddington, C.S. Wilcox, Tetrahedron Lett. 41 (1992) 6085.
[36] E. Fan, S.A. van Arman, S. Kincaid, A.D. Hamilton, J. Am. Chem. Soc. 115 (1993) 369.
[37] M. Boiocchi, L. Del Boca, D. Esteban-Gómez, L. Fabbrizzi, M. Licchelli, E. Monzani, J. Am. Chem. Soc. 126 (2004) 16507.
[38] G.A. Jeffrey, An Introduction to Hydrogen Bonding, Oxford University Press, Oxford, 1997.
[39] T. Steiner, Angew. Chem., Int. Ed. 41 (2002) 48.
[40] S. Gronert, J. Am. Chem. Soc. 115 (1993) 10258.
[41] M. Boiocchi, L. Del Boca, D. Esteban-Gómez, L. Fabbrizzi, M. Licchelli, E. Monzani, Chem. Eur. J. 11 (2005) 3097.
[42] F.G. Bordwell, Acc. Chem. Res. 21 (1988) 456.
[43] D. Esteban-Gómez, L. Fabbrizzi, M. Licchelli, E. Monzani, Org. Biomol. Chem. 3 (2005) 1495.
[44] V. Amendola, D. Esteban-Gómez, L. Fabbrizzi, M. Licchelli, E. Monzani, F. Sancenón, Inorg. Chem. 44 (2005) 8690.
[45] M.W. Glenny, L.G.A. Van de Water, W.L. Driessen, J. Reedijk, A.J. Blake, C. Wilson, M. Schroeder, Dalton Trans. 13 (2004) 1953.
[46] B.D. Smith, J.M. Mahoney, Encyclopedia of Supramolecular Chemistry, Marcel Dekker, New York, 2004, p. 1291.
[47] J.M. Mahoney, A.M. Beatty, B.D. Smith, J. Am. Chem. Soc. 123 (2001) 5847.
[48] H. Miyaji, W. Sato, J.L. Sessler, Angew. Chem., Int. Ed. 39 (2000) 1777.
[49] T. Mizuno, W.-H. Wei, L.R. Eller, J.L. Sessler, J. Am. Chem. Soc. 124 (2002) 1134.
[50] Y. Kubo, M. Yamamoto, M. Ikeda, M. Takeuchi, S. Shinkai, S. Yamaguchi, K. Tamao, Angew. Chem., Int. Ed. 42 (2003) 2036.
[51] S. Kondo, M. Nagamine, Y. Yano, Tetrahedron Lett. 44 (2003) 8801.
[52] S. Solé, F.P. Gabbaï, Chem. Commun. (2004) 1284.
[53] L. Zhou, X. Zhang, S. Wu, Chem. Lett. 33 (2004) 850.
[54] T. Ghosh, B.G. Maiya, M.W. Wong, J. Phys. Chem. A 108 (2004) 11249.
[55] R. Miao, Q.-J. Zheng, C.-F. Chen, Z.-T. Huang, Tetrahedron Lett. 45 (2004) 4959.
[56] D.A. Jose, D.K. Kumar, B. Ganguly, A. Das, Org. Lett. 6 (2004) 3445.
[57] J.Y. Lee, E.J. Cho, S. Mukamel, K.C. Nam, J. Org. Chem. 69 (2004) 943.
[58] J.Y. Kwon, Y.J. Jang, S.K. Kim, K.-H. Lee, J.S. Kim, J. Yoon, J. Org. Chem. 69 (2004) 5155.
[59] V. Thiagarajan, P. Ramamurthy, D. Thirumalai, V.T. Ramakrishnan, Org. Lett. 7 (2005) 657.
[60] D. Esteban-Gómez, L. Fabbrizzi, M. Licchelli, J. Org. Chem. 70 (2005) 5717.